African Journal of Pharmaceutical Research and Development
Available online at https://ajopred.com
Vol. 18 No.1; pp. 417-445 (2026)

Original Research Article

METHANOL EXTRACT OF *Ficus platyphylla* AMELIORATES THE SEVERITY OF LITHIUM-PILOCARPINE-INDUCED STATUS EPILEPTICUS IN RATS

BEN AHMED CHINDO[1,2*], MUSA ITOPA YAKUBU[1], ABDULFATAI ADETUNJI JIMOH[1], NEWTHING SIMON SHUAIBU[1], IDRIS ABDULLAHI[3], PETER MAITALATA WAZIRI[4], STEPHEN AMONG JAMES[4], GODWIN IKO AYUBA[5], ZAKARI LADAN[6,8], SAMSON AMOS[7]

1. Department of Pharmacology and Toxicology, Faculty of Pharmaceutical Sciences, Kaduna State University, Kaduna, Nigeria,
2. Department of Pharmacology and Toxicology, Faculty of Pharmaceutical Sciences, Federal University of Applied Sciences, Kachia, Nigeria,
3. Department of Pharmaceutical and Medicinal Chemistry, Faculty of Pharmaceutical Sciences, Kaduna State University, Kaduna, Nigeria
4. Department of Biochemistry, Faculty of Life Sciences, Kaduna State University, Kaduna, Nigeria
5. Department of Anatomic Pathology and Forensic Medicine, College of Medicine, Kaduna State University, Kaduna, Nigeria
6. Department of Chemistry, Faculty of Physical Sciences, Kaduna State University, Kaduna, Nigeria
7. School of Pharmacy, Cedarville University, Ohio, USA
8. Department of Industrial Chemistry, Faculty of Science, Federal University of Applied Sciences, Kachia, Nigeria

ABSTRACT

Pilocarpine model of epilepsy reproduces features of temporal lobe epilepsy (TLE) associated with mossy fiber sprouting, gliosis, and extensive loss of dentate gyrus and hippocampal pyramidal neurons. TLE is often resistant to drug treatment, proceeding from impaired mitochondrial energy production and failure of GABAergic inhibition. In this study, *Ficus platyphylla* (FP) was extracted with methanol and the methanol extract subjected to Gas Chromatographic-Mass Spectrometric (GC-MS) and Fourier-transform infrared spectroscopic (FT-IR) analyses. *In silico* molecular docking study was conducted to predict interactions of the major compounds from FP with glutamic acid decarboxylase (GAD) and γ-aminobutyric acid aminotransferase ($GABA_{AT}$). Effects of FP on lithium-pilocarpine-induced status epilepticus (SE) and neuronal cell damage were examined, and the involvement of oxidative and GABAergic pathways investigated to define the likely target(s) for development of the bioactive components. FP at doses of 50, 100 and 200 mg/kg, protected 8%, 27% and 20% of rats from lithium-pilocarpine-induced status epilepticus (SE), respectively. FP alleviated lithium-pilocarpine-induced seizure severity ($p < 0.01$) and extended the latencies to seizures ($p < 0.001$) and SE ($p < 0.001$) in non-protected rats. The extract ameliorated neuronal cell damage and *oxidative stress induced by* lithium-pilocarpine administration. FP significantly ($p < 0.001$) increased *the expression of genes encoding* glutathione-S-synthase (GSS), superoxide dismutase (SOD), catalase (CAT), and glutamic acid decarboxylase (GAD). The major compounds in the extract including octadecenoic acid, dimethylphenylisothiocyanate, and pentadecanoic acid showed interaction with GAD and $GABA_{AT}$ active sites. These preliminary findings revealed the ameliorative effects of FP against lithium-pilocarpine-induced status epilepticus, neuronal cell damage and alterations of oxidative stress biomarkers. Bioactive compounds in the extract interacted with GAD and $GABA_{AT}$ active sites. Further studies are required to unravel the potential values of bioactive constituents of FP for the management of temporal lobe epilepsy.

ARTICLE INFO

Received 20 February 2026
Accepted 26 April, 2026
Published 30 April 2026

KEYWORDS

Ficus platyphylla,
Lithium-pilocarpine,
Status epilepticus,
Neuronal cell damage,
GABAergic pathways,
oxidative pathways

***Corresponding author:** bachindo@kasu.edu.ng, +234 803 289 9112

https://doi.org/10.59493/ajopred/2026.1.3 ISSN: 0794-800X (print); 1596-2431 (online)

INTRODUCTION

Epilepsy is a multifaceted brain disorder characterized by periodic interruptions of normal brain function caused by an excessive, sudden or rapid discharge of cerebral neurons in the grey matter of the brain, culminating in brief episodes of partial or generalized involuntary movement that may be accompanied by loss of consciousness [1]. This family of chronic neural disorders that commonly increased predisposition to seizures to reflect underlying brain dysfunction [1], may result from defects in membrane ATPase, potassium conductance and ion channels linked to neuronal membrane instability; metabolic, infectious, deformed, vascular, traumatic or tumoral, conditions [2].

Status epilepticus (SE) is a state of prolonged seizure activity that lasts for at least 30 minutes without regaining full consciousness between the seizure episodes [3]. This paroxysmal neurological crisis associated with significant mortality and morbidity, results from a failure of inhibitory pathways mediated by γ–aminobutyric acid (GABA) or increased excitatory neurotransmission mediated by glutamate [3, 4, 5, 6]. Excessive glutamatergic and loss of GABAergic neurotransmissions are implicated in the pathophysiology of SE, and models of SE essentially provide insights into the pathogenesis of TLE [7]. High-dose pilocarpine and Lithium-pilocarpine models reproduce many features of TLE in rodents, which include an initial triggering of brain injury, culminating in epileptic foci in the limbic system; followed by a latent period and later by the appearance of spontaneous recurrent seizures (SRSs), and reorganization of neuronal networks resulting from the presence of hippocampal sclerosis [7, 8]. SE is associated with impaired mitochondrial dynamics, bioenergetic failure and oxidative stress in both immature and mature brains [9].

Oxidative stress and mitochondria dysfunction are critical elements in the pathophysiology of epilepsy. Dysfunction of mitochondrial calcium buffering, ATP generation, and the regulation of apoptosis are crucial factors in the onset and course of epilepsy [10]. Clinical and experimental data have established the fundamental role that oxidative stress plays in the initiation and progression of epilepsy [11]. Oxidative stress results from an imbalance between potential of antioxidant defenses and pro-oxidant species, culminating in oxidative damage to DNA, lipids and proteins, resulting to apoptosis and cellular damage [12]. Oxidative stress can further impair mitochondrial function resulting to metabolic disturbances in neurons [9]. Reactive oxygen species (ROS) and reactive nitrogen species (RNS) are free radicals produced in the body as byproducts of cellular metabolism [13, 14], which can become harmful when produced in excess [15]. Elevations in levels of malondialdehyde (MDA), a marker of lipid peroxidation have been observed in patients with recurrent seizures [16]. Decreased levels of antioxidant enzymes including catalase (CAT) and superoxide dismutase (SOD), together with elevated levels of MDA, are suggestive that the antioxidant defense system is overcome by ROS production [16].

Recent advances have highlighted the potential of antioxidant therapy as a novel treatment strategy of epilepsy [9]. Neuroprotectants, particularly antioxidants, may have therapeutic value in epilepsy by reducing oxidative stress and its damaging effects on neurons. Increased levels of antioxidant enzymes such as SOD, CAT, and glutathione (GSH) have been proposed as potential therapeutic targets in refractory epilepsy [9, 17]. Targeting oxidative stress and mitochondrial dysfunction represents a promising adjunctive strategy to modify the progression and improve therapeutic outcomes for epileptics. Synergistic effects can be achieved by combining antioxidants that target multiple pathways, modulating neurotransmitter systems, reducing oxidative stress, and attenuating neuroin**fl**ammation.

Temporal Lobe Epilepsies are refractory to standard anti-epileptic drug (AED) treatment. Impairment in mitochondrial energy production is believed to the basis of pharmacoresistance in epilepsy [9]. Moreover, these traditional anticonvulsant medications commonly employed in the management of TLE cause devastating side effects without improvement in the patient's quality of life. Although, surgical interventions are currently the options used to achieve seizure control in TLE [18, 19], research is ongoing to develop new anticonvulsant drugs that are available, affordable, and effective to overcome these impediments. Plants are the main sources of lead compounds and novel medications for the management of this devastating brain condition [20, 21, 22, 23]

Ficus platyphylla Del.-Holl, *an ethnomedicinal shrub belonging to the family moraceae, is indigenous to the savanna localities of the coast of West Africa.* Extracts from *Ficus platyphylla* are utilized in Nigerian folk medicine to manage inflammation, pain, psychoses, depression and epilepsy. Our earlier studies revealed the potential anticonvulsant values [2, 24, 25, 26] and safety [27] of this ethnomedicinal plant, which validates its utilizations in the Nigerian traditional medicine for the

treatment of epilepsy. To complement our earlier findings on the antiepileptic potentials of *Ficus platyphylla*, we examined its ameliorative properties against lithium-pilocarpine induced status epilepticus and alterations of biomarkers of oxidative stress in rats. We also conducted *in silico* molecular docking analysis to predict interactions between the major bioactive compounds form FP and two enzymatic drug targets for the treatment of epilepsy.

MATERIALS AND METHODS

Animals

Male and female Wister rats (180-200 g), aged 8–9 weeks fed with normal feeds and water *ad libitum*, were obtained from the Kaduna State University's (KASU's) Animal House. The rats were accommodated in clear plastic cages cushioned with wood shavings, under normal conditions of light/dark cycles (12/12 h), temperature (22 ± 1°C) and humidity. The number of rats approved by the Animal Ethics Committee of KASU (No. KASU/AEC/2023/005) for this study were used according to guidelines for the use and care of laboratory animals (updated 2011) prescribed by the National Institute of Health's (NIH Publications No. 80-23).

Plant Collection and Preparation of the Extract

The FP was identified, collected, cleaned and authenticated *by Mallam Ibrahim Muazzam, National Institute for Pharmaceutical Research and Development (NIPRD), Abuja, Nigeria; and a voucher specimen (No. 4035) is placed in NIPRD Herbarium for future reference. The bark was* sliced into pieces, air dried, crushed with pestle and mortar, and extracted with methanol. The preliminary phytochemical and HPLC analysis of the extract have been conducted and reported by Chindo *et al*. [25].

High Performance Liquid Chromatographic (HPLC), Gas Chromatography-Mass Spectrometric (GC-MS), and Fourier-Transform Infrared Spectroscopic (FT-IR) analysis

Here, we used the ultra-model Shimadzu GC-MS QP2010, as previously described by Beschi *et al* [28] to analyze the methanol extract of FP. Helium with a split ratio of 10:1 (99.999%) and a constant flow rate of 1 ml/minute was used as the carrier gas. A single microliter of sample was injected into the Column Elite-1 fused silica capillary column (30×0.25 mm ID×0.25µm) with an electron impact mode of 70 eV. The injector and ion source temperatures were set at 250°C. The oven was programmed to begin at 110°C (isothermal for 2 minutes), increased by 10°C per minute to 200°C and eventually increased by 5°C every 15 minutes to 260°C (isothermal). Mass spectra were acquired at 70 eV with a 0.5-second scan interval and fragmented in the range of 40 to 550 Da for approximately 30 minutes. The GC-MS data was processed using electron impact ionization at 70 eV, and the total ion count (TIC) was utilized to evaluate the data for compound identification and quantification. NISP Search was used to compare the component spectrums to the GC-MS library's database of known spectra. The relative percentage quantity was calculated by comparing the average peak area of each component to the total area. The Turbo-Mass-OCPTVS-Demo SPL application was used to process data and measure peak areas. The Fourier-transform infrared spectroscopy (FT-IR) spectra were run with the Perkin Elmer Spectrophotometer system (PerkinElmer, Waltham, MA, USA), and the spectra scanned from 4000cm^{-1} to 400 cm^{-1}.

Lithium-pilocarpine status epilepticus induction

Rats were randomly selected, divided into five experimental groups and treated with saline and FP (50, 100 and 200 mg/kg) orally for three days before SE induction [29]. A significant decrease in the dosage of pilocarpine was achieved by administering Lithium Chloride (Li, 127 mg/kg) eighteen hours before SE induction [30]. On the fourth day, the rats were treated with saline and FP (50, 100 and 200 mg/kg) orally 1 h prior to SE induction. Hyoscine (1mg/ml, *i.p*) was administered 30 minutes prior to SE induction to reduce peripheral cholinergic activity associated with pilocarpine injections [31, 32]. Following administration of pilocarpine (40 mg/kg, i.p.) to induce SE, the animals were closely monitored for signs of seizure activity using a modified version of Racine's scale as follows: 1 = for infrequent face clonus and immobility; 2 = head nodding; 3 = rearing; 4 = rearing and tumbling on both sides; and 5 = for tonic hind limbs extension. These steadily progressed into SE within 1-2 h [33] with SE defined as uninterrupted seizures lasting for more than 30 minutes after pilocarpine injection [34, 35]. To reduce excitability after 2 h of SE, the rats were injected with 4 mg/kg of diazepam; and phenobarbitone (30 mg/kg) injected forty-five minutes later to block the residual seizure activity [36].

Biochemical Studies

Rats were decapitated after euthanasia with ether. The brains were rapidly removed and homogenized in phosphate buffer prior to centrifuging at 4°C for 10 minutes at 10, 000 rpm. The following biochemical tests were conducted. The test described by Moron *et al*. [37] was utilized to evaluate the *Glutathione* levels. The

absorbance of a yellow chromophore obtained from the reaction of DTNB [5, 5–dithiobis-(2-nitrobenzoic acid)] and brain tissues was *assessed at 412 nm alongside a blank reagent* (DTNB + phosphate buffer) to give the reduced glutathione levels. The thiobarbituric acid test described by Ohkawa *et al*. [38] was applied to estimate the concentrations of *Malondialdehyde*. A pink supernatant was obtained and its absorbance was assessed at 532 nm with distilled water as reference blank. The method described by Misra and Fridovich [39] was used to assess *superoxide dismutase* (SOD) activity. An adrenochrome was obtained from the mixture of adrenaline solution (1.3 mM) and EDTA (0.6 mM) with the supernatant solution, and the adrenochrome's absorbance was assessed at 480 nm alongside the chemicals put together without the tissue homogenate as blank sample. The method described by Góth [40] was used to evaluate *catalase* activity. A mixture of the tissue homogenate and potassium phosphate buffer was added to thirty millimoles hydrogen peroxide (H_2O_2) in 50 mM potassium phosphate buffer to recruit a reaction; the absorbance was evaluated at 240 nm, and activity presented as 1 µmol H_2O_2 decomposed U/mg protein.

Histology evaluation

The method described by Chindo *et al*. [26] was used with modifications to prepare the brains for analysis. The rats were beheaded under anesthesia, the brains were quickly removed and preserved in Bouin's fluid for 16–24 h. The brains were processed and fixed in paraffin, and 5 µm thick sections were made with a rotary microtome. The sections were stained with Nisl stain. The neurons in fields (500 µm by 500 µm) of the hippocampal CA1 and CA3 regions were counted using a counting net. An average of five squares were counted in the left and right hippocampal regions of each rat.

Gene expression studies

The relative changes in gene expression from real-time quantitative PCR experiments were analyzed using the 2(-Delta Delta CT)) method [41, 42]. Primers for gene expression were designed on the NCBI website with primer blast software and their sequences were synthesized by Integrated DNA Technologies (IDT), Singapore. RNAs were isolated from brain tissue samples using TRIpure Total RNA Extraction Reagent (ELK Biotechnology, USA) and transcribed into cDNA using ReverTra Ace™ qPCR RT Master Mix with gDNA Remover (Toyobo, Japan) [43]. The DNase 1 reaction solution containing 2 µL of nuclease, 6 µL of RNA template (80 µg/mL) and 2 µL of 4x DN master mix free water was prepared for genomic DNA remover and incubated for 5 min at 37°C. Thereafter, incubated serially at 37°C for 15 min, 50°C for 5 min and finally at 98°C for 5 min to terminate the reaction after the addition of 2 µL of 5x RT master mix II. The cDNA synthesized was stored at -20°C for further assay.

Quantitative Real-Time PCR (qRT-PCR) analysis

Expression of the target genes was measured by qRT-PCR using Luna universal qPCR master mix (M3003). The PCR was done using the synthesized cDNA as described in the Manufacturer's protocol. The conditions were set as follows; initial denaturation at 95°C for 60 seconds, followed by 2-step cycle of 95°C for 15 seconds and 55°C for 30 seconds. Relative quantification was determined by normalizing the cycle threshold (CT) of target genes with the CT of beta-actin (control gene) using the $2^{-\Delta\Delta CT}$ method.

Table 1: Primer Sequences of Genes.

Gene	Forward sequence	Reverse sequence
GSS	TTTGACCAGCGTGCCGTAGA	GGGCATGTAGCCATCTCGGA
SOD	TCCGTCGGCTTCTCGTCTTG	CCGCTTTCATCGCCATGCTT
CAT	GAGTGGCCAACTACCAGCGT	TGTCCGCACCTGAGTGACAT
GAD	CCGCAGGCACGACTGTTTAC	GGGACATGAGCAGTCCACCA

GSS –Glutathione Synthetase, SOD – Superoxide Dismutase, CAT –Catalase,
GAD –Glutamic Acid Decarboxylase

Molecular docking studies

In silico molecular docking analysis was performed following established protocols [44, 45] to predict the interactions of 2,3-Dimethylphenylisothiocyanate, Pentadecanoic acid, and 11-Octadecenoic acid with target proteins that are implicated in neurotransmitter metabolism. The 3D structures of the ligands were retrieved from the PubChem database [46] and were further converted into mol2 format using OpenBabel [47]. Protein structures of gamma-aminobutyric acid aminotransferase ($GABA_{AT}$, PDB ID: 1OHV) and glutamic acid decarboxylase (GAD, PDB ID: 2OKJ) were obtained from the RCSB PDB database (https://www.rcsb.org/structure/). Preprocessing was

carried out using AutoDock Tools 4.2 [48] by adding hydrogen atoms, assigning Kollman charges, and removing crystallographic water molecules. To validate the docking protocol, the co-crystallized ligands–pyridoxal-5'-phosphate (PLP) in 1OHV and 4-[({3-hydroxy-2-methyl-5 [(phosphonooxy) methyl] pyridin-4-yl} methyl) amino] botanic acid (PLZ) in 2OKJ–were re-docked into their respective binding sites. The docking successfully reproduced the native binding conformations, confirming the reliability of the docking parameters. This re-docking served as a benchmark for comparison with the test compounds, thus, fulfilling the requirement for rigorous validation [45]. For each ligand (2, 3-Dimethylphenylisothiocyanate, Pentadecanoic acid, and 11-Octadecenoic acid), torsional flexibility and Gasteiger charges were assigned. Docking simulations were executed using the Lamarckian Genetic Algorithm with 100 independent runs per ligand. The best-scoring conformations were selected from clustering analysis based on binding free energy. Docking results of the test ligands were systematically compared with the validated re-docked controls (PLP and PLZ) in terms of binding energies, hydrogen bonding, and hydrophobic interactions. This comparative framework allowed assessment of the test ligands relative to established inhibitors, ensuring methodological rigor. The final docked complexes were analyzed using Protein-Ligand Interaction Profiler (PLIP) [49] and ProteinPlus server [50, 51, 52] for detailed characterization of hydrogen bonds, hydrophobic interactions, and other non-covalent forces.

Statistical Analysis

Data were presented as mean ± S.E.M. and analyzed by one-way ANOVA, followed by Turkey post hoc tests using Graph Prism version 4.00 (GraphPad Software, Inc., La Jolla, CA, USA), with significant results at $p < 0.05$. n = represents the number of animals per group for each experiment.

RESULTS

Bioactive constituents of methanol extract of *Ficus platyphylla* (FP)

Twenty biologically active secondary metabolites were detected in FP by GC-MS analysis with the major compounds being pentadecanoic acid (13.10%), 2, 3-dimethylphenylisothiocyanate (13.47%) and 11-Octadecenoic acid (14.35%) [(Table 2; Chromatograms of these most abundance secondary metabolites are shown in Figure 1 (A–C)]. The FT-IR spectral data revealed the following major functional groups: broad hydroxyl, $O\text{-}H_{str}$ ($3200cm^{-1}$), sharp $C\text{-}H_{str}$ ($2980cm^{-1}$), sharp C=Ostr ($1730cm^{-1}$) corresponding to carbonyl functional group and a strong C=C str ($1602cm^{-1}$) peak. These functional groups may probably be from the major constituents (11-Octadecenoic acid, methyl ester, Pentadecanoic acid and 14-methyl-, methyl ester compounds (Figure 1D).

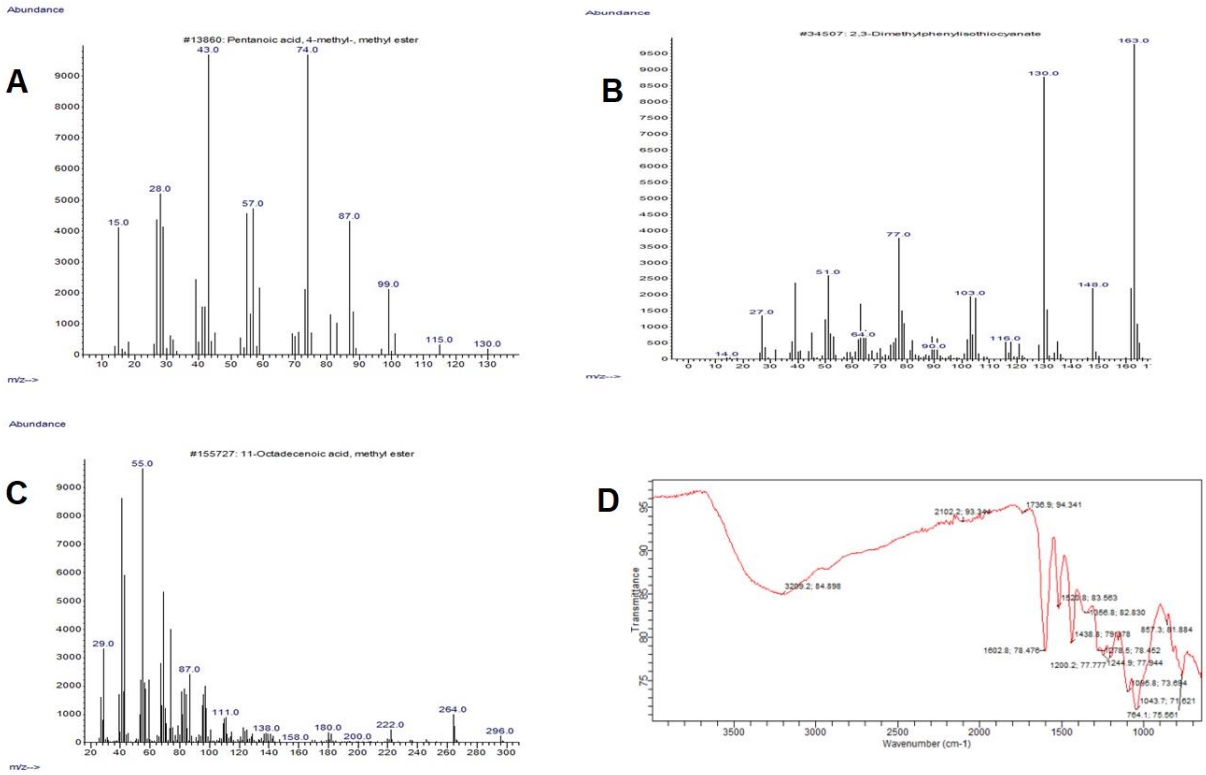

Figure 1. Mass spectra of (A) Pentadecanoic acid; (B) 2, 3-dimethylphenylisothiocyanate and (C) 11-Octadecenoic acid from methanol extract of *Ficus platyphylla*. (D) Fourier-transform infrared spectroscopy (FT-IR) spectra of the methanol extract of *Ficus platyphylla* was run with Perkin Elmer Spectrophotometer system (PerkinElmer, Waltham, MA, USA), and the spectra scanned from 4000cm^{-1} to 400cm^{-1}.

Table 2: GC-MS data showing the Chemical constituents in *Ficus platyphylla* and their percentage compositions

Compound	Retention time (min)	Percentage composition	Structure
9-Oxabicyclo[6.1.0]nonane, cis-	5.1549	5.6439	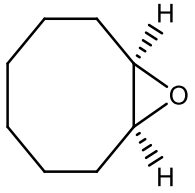
Ethanamine, 2-chloro-N,N-dimethyl-	12.0085	7.5948	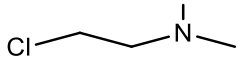
2-Isoxazoline, 3-phenyl-	14.9849	9.0912	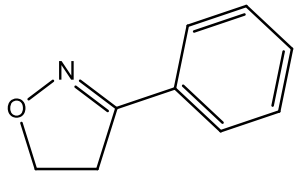

Benzenemethanol, 2-nitro-	15.6483	7.4515	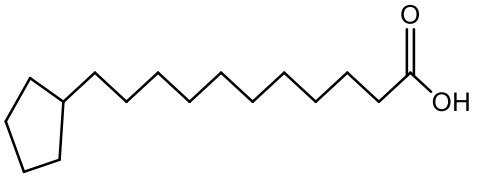
2-Propenoic acid, 3-phenyl-	15.9266	2.8909	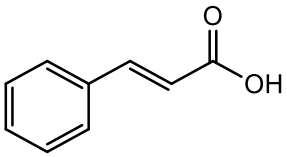
2-Isoxazoline, 3-phenyl-	16.1104	3.4859	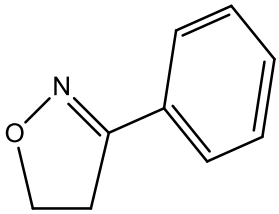
2-Propenoic acid, 3-phenyl-	16.3691	1.9825	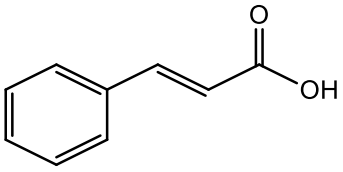
2-Propenoic acid, 3-phenyl-	16.8548	2.3066	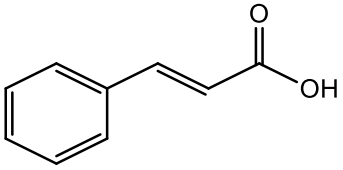
2-Propenoic acid, 3-phenyl-	17.0291	0.4334	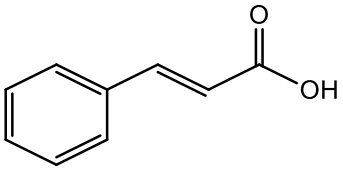
2-Propenoic acid, 3-phenyl-	17.3589	1.1245	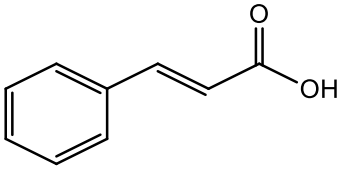
trans-Cinnamic acid	17.6838	1.0142	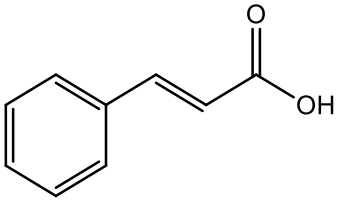

2,3-Dimethylphenylisothiocyanate	19.6846	13.473	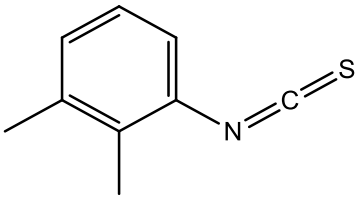
Pentadecanoic acid, 14-methyl-, methyl ester	20.246	13.1004	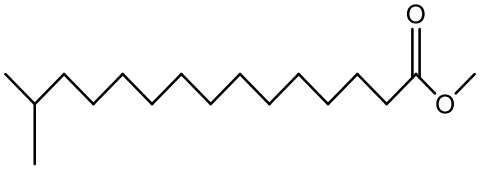
3,4-Octadiene, 7-methyl-	23.3196	4.5576	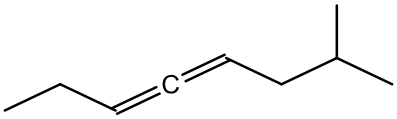
11-Octadecenoic acid, methyl ester	23.4912	14.3511	
Pentanoic acid, 4-methyl-, methyl ester	24.0854	1.5221	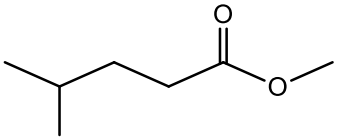
Cyclopentaneundecanoic acid	26.4721	1.0818	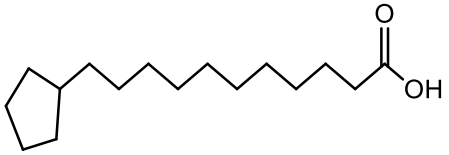
Cyclopentaneundecanoic acid	26.8739	0.4051	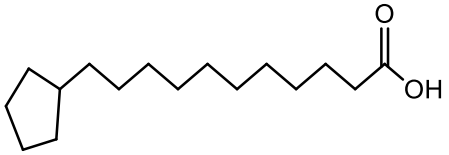
Cyclopentaneundecanoic acid	29.329	3.0758	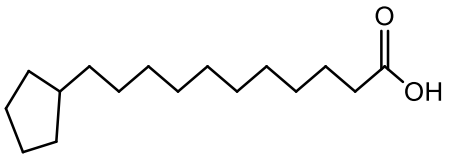
Permethrine	33.2247	5.4139	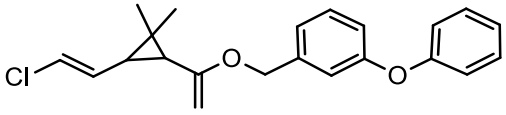

NISP Search was used to compare the component spectrums to the GC-MS library's database of known component spectrums. The relative percentage quantity was calculated by comparing the average peak area of each component to the total area.

Lithium–pilocarpine status epilepticus

The rats showed immobility; face clonus, head nodding; rearing and tumbling, which steadily progressed to generalized seizures after lithium-pilocarpine injection, culminating into status epilepticus (SE). FP treatment dose-dependently protected rats from lithium-pilocarpine-

induced status epilepticus (SE) and significantly ($F_{3, 56}$ = 19.91, p < 0.0001; ***p < 0.001) increased the Latency to status epilepticus in the non-protected rats. FP significantly ($F_{3, 40}$ = 17.17, p < 0.0001; ***p < 0.001) increased the Latency to seizures; and ameliorated seizure severity ($F_{3, 57}$ = 5.704, p = 0.0018; **p < 0.01) in a dose dependent manner (Figure 2).

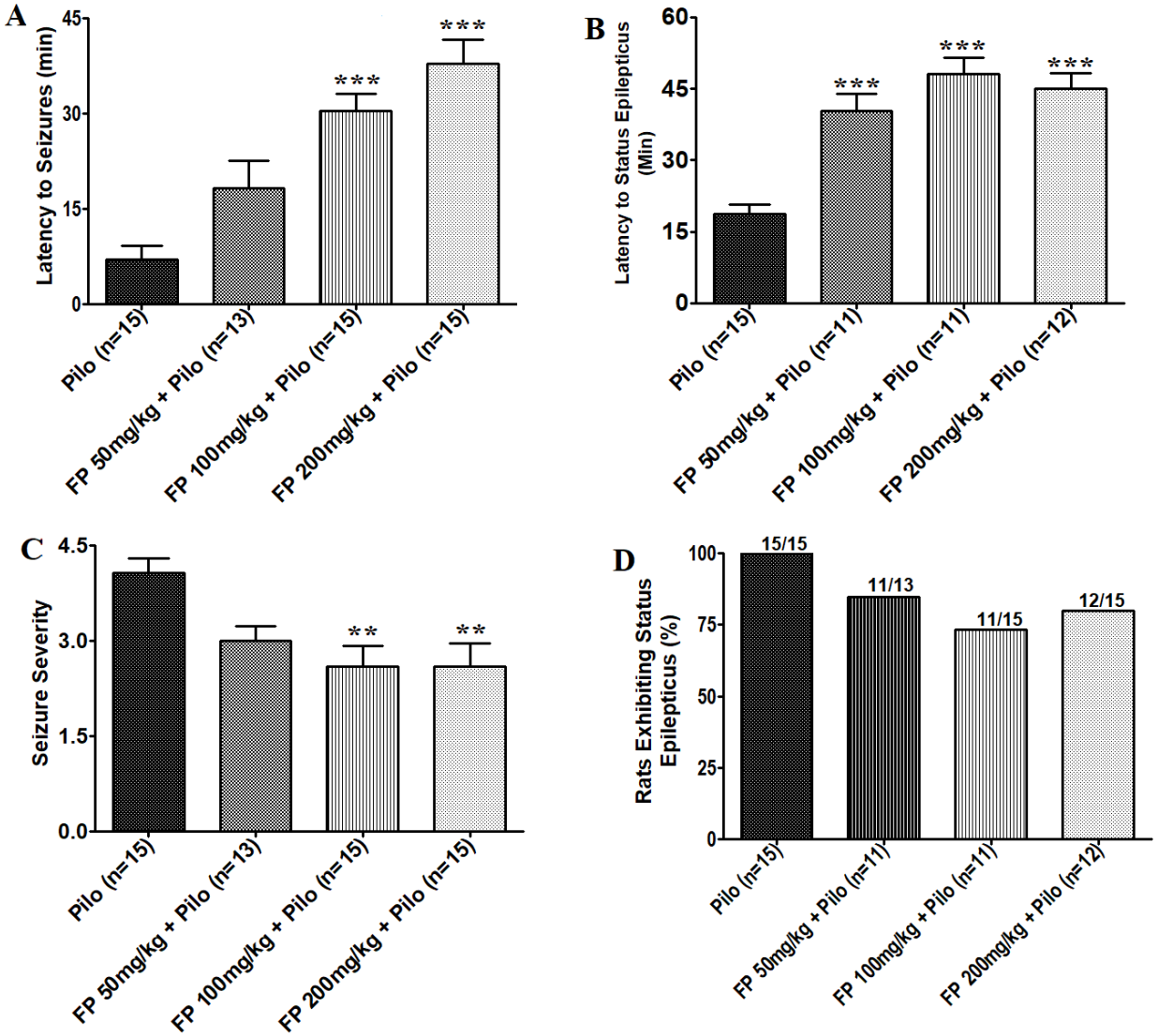

Figure 2: Effects of *Ficus platyphylla* (FP) on lithium-pilocarpine-induced status epilepticus (SE) in rats. (A) Latency to seizures [($F_{3, 40}$ = 17.17, p < 0.0001; ***p < 0.001 (Pilo vs FP 100mg/kg + Pilo; Pilo vs FP 200mg/kg + Pilo)]; (B) Latency to status epilepticus [($F_{3, 56}$ = 19.91, p < 0.0001; ***p < 0.001 (Pilo vs FP 50mg/kg + Pilo; Pilo vs FP 100mg/kg + Pilo; Pilo vs FP 100mg/kg + Pilo)]; (C) Severity of seizures [($F_{3, 57}$ = 5.704, p = 0.0018; **p < 0.01 (Pilo vs FP 100mg/kg + Pilo; Pilo vs FP 200mg/kg + Pilo)]; (D) Percentile of rats that exhibited SE. Data expressed as Mean± SEM. n = number of animals per group.

Biochemical studies

Glutathione (GSH) levels significantly ($F_{4, 27}$ = 8.060, p = 0.0003; ++p < 0.01) depleted in lithium–pilocarpine (Li–Pc) group and pretreatment with FP insignificantly increased the GSH levels compare to the Li–Pc group (Figure 3A). Malondialdehyde (MDA) levels markedly ($F_{4, 29}$ = 4.299, p = 0.0088; ++p < 0.01) increased in rats treated with Li–Pc only group, and pretreatment with FP attenuated the increase of MDA levels induced by Li–Pc (Figure 3B). Superoxide dismutase (SOD) activity significantly ($F_{4, 27}$ = 8.162, p = 0.0003; +++p < 0.001) decreased in rats treated with Li–Pc only and pretreatment with FP markedly ($F_{4, 27}$ = 8.162, p = 0.0003; **p < 0.01) increased SOD activity compared to the Li–Pc group (Figure 3C). Catalase (CAT) activity significantly ($F_{4, 23}$ =10.18, p = 0.0001; ++p < 0.01) decreased in the group treated with

Li–Pc only and pretreatment with FP markedly ($F_{4, 23}$ =10.18, p = 0.0001; ***p < 0.001) improved catalase activity (Figure 3D).

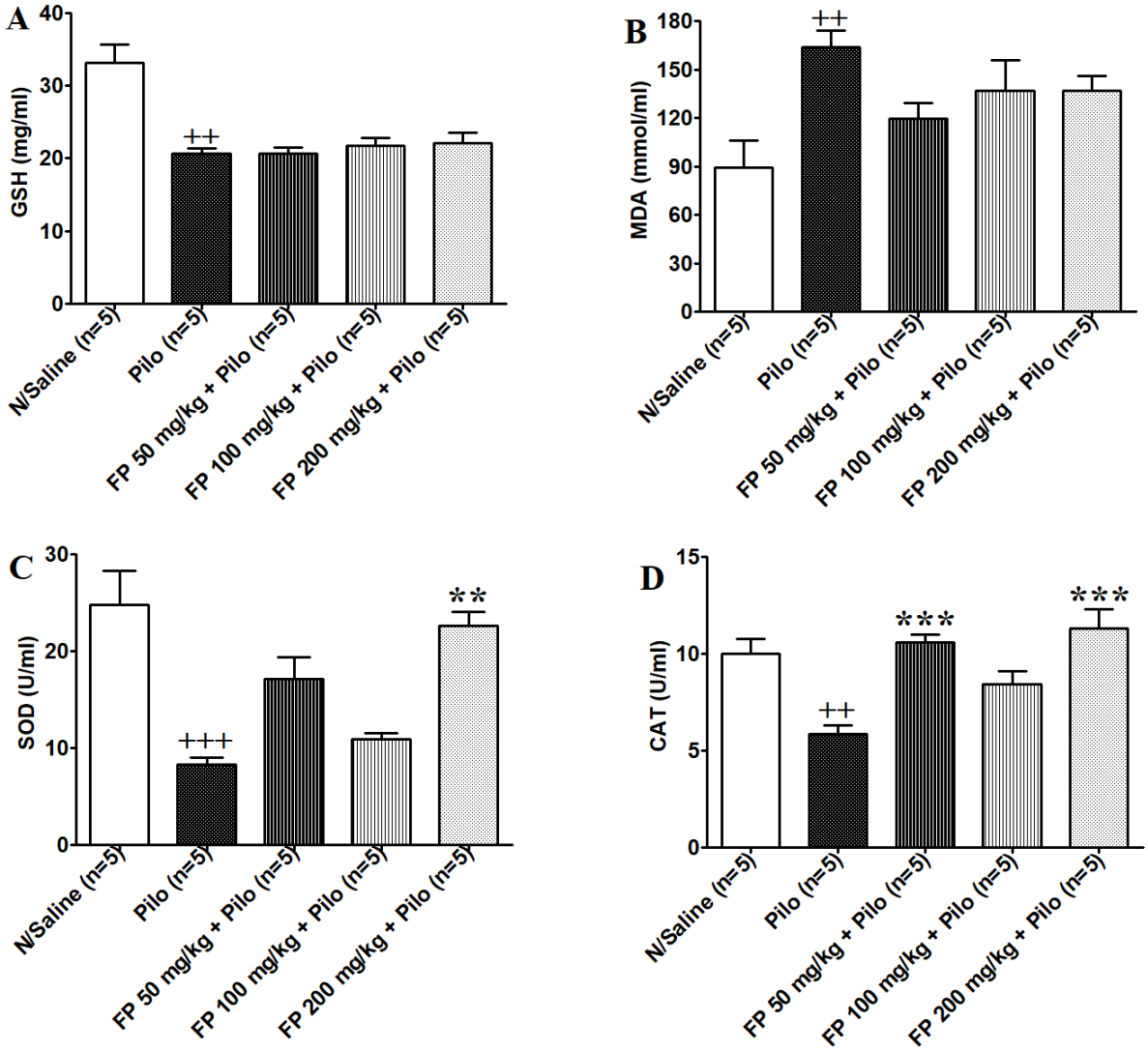

Figure 3: Effects of *Ficus platyphylla* (FP) on oxidative stress markers in rats' brains after lithium-pilocarpine-induced status epilepticus (SE). (A) Glutathione (GSH) levels [($F_{4, 27}$ = 8.060, p = 0.0003; ++p < 0.01 (N/Saline vs Pilo)]; (B) Malondialdehyde (MDA) levels [($F_{4, 29}$ = 4.299, p = 0.0088; ++p < 0.01 (N/Saline vs Pilo)]; (C) Superoxide dismutase (SOD) activity [($F_{4, 27}$ = 8.162, p = 0.0003; +++p < 0.001 (N/Saline vs Pilo), **p < 0.01 (Pilo vs FP 200 mg/kg + Pilo)]; (D) Catalase (CAT) activity [($F_{4, 23}$ =10.18, p = 0.0001; ++p < 0.01 (N/Saline vs Pilo), ***p < 0.001 (Pilo vs FP 50 mg/kg + Pilo; Pilo vs FP 200 mg/kg + Pilo)]. Data expressed as Mean ± SEM. n = number of animals per group.

Gene expression (qPCR) analysis

Treatment with FP significantly increased the expression of genes encoding glutathione-S-Synthase (GSS) ($F_{3, 19}$ = 30.92, p < 0.0001; ***p < 0.001) (Figure 4A); superoxide dismutase (SOD) ($F_{3, 19}$ = 95.05, p < 0.0001; *p < 0.05, ***p < 0.001) (Figure 4B); catalase (CAT) ($F_{3, 19}$ = 460.4, p < 0.0001; ***p < 0.001) (Figure 4C); and glutamic acid decarboxylase (GAD) ($F_{3, 19}$ = 552.0, p < 0.0001; ***p < 0.001) compared to the Li–Pc group (Figure 4D).

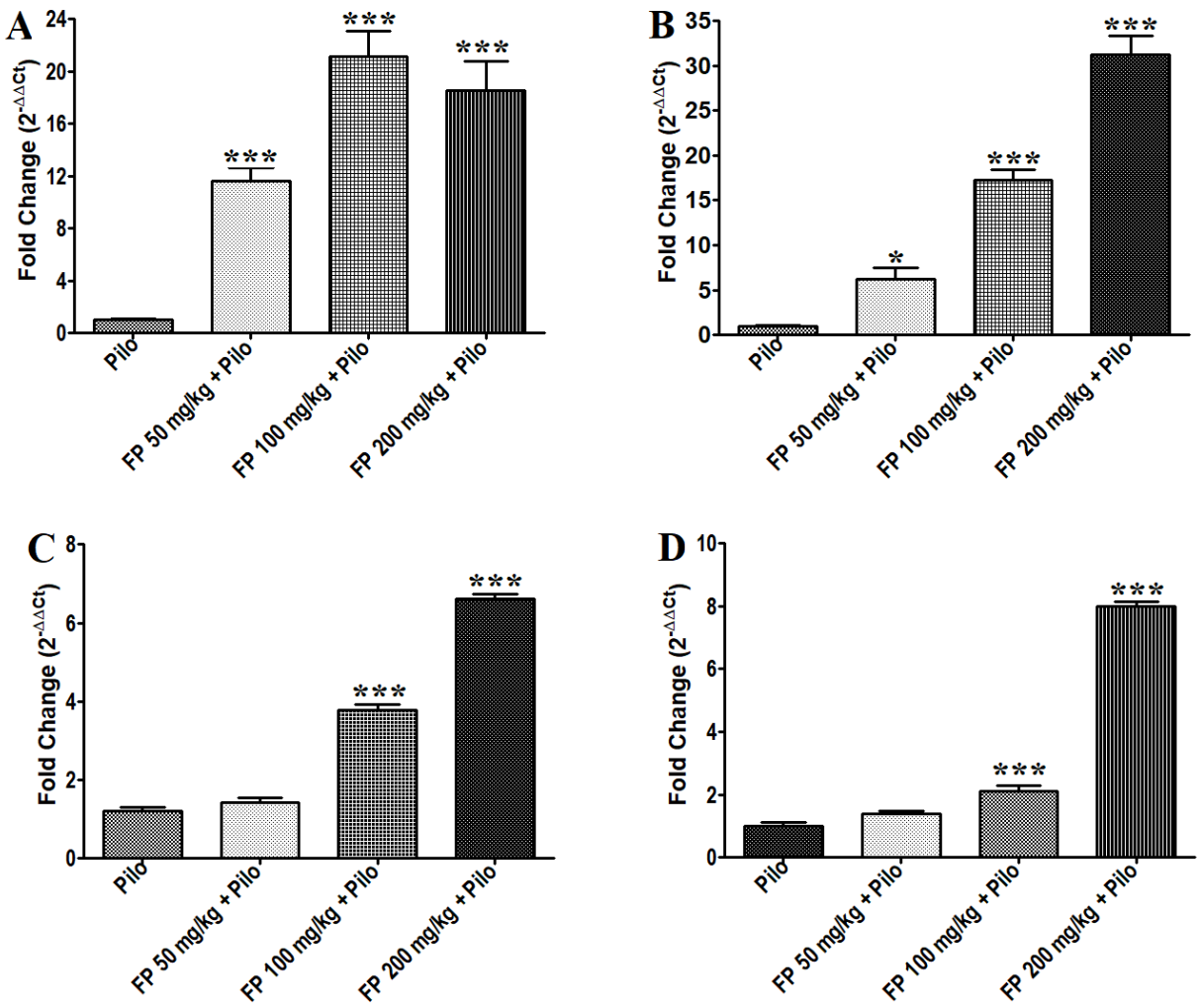

Figure 4: Fold changes in gene expression using $2^{-\Delta\Delta Ct}$ method. (**A**) Glutathione-S-Synthase (GSS) ($F_{3, 19}$ = 30.92, p < 0.0001; ***p < 0.001); (**B**) Superoxide dismutase (SOD) [($F_{3, 19}$ = 95.05, p < 0.0001; *p < 0.05, ***p < 0.001)]; (**C**) Catalase (CAT) [($F_{3, 19}$ = 460.4, p < 0.0001; ***p < 0.001)]; (**D**) Glutamic acid decarboxylase (GAD) [($F_{3, 19}$ = 552.0, p < 0.0001; ***p < 0.001)]. Data expressed as Mean ± SEM. n = 5 per group.

Histological analysis

The hippocampi of rats in the normal saline group presented normal neural processes and neuronal cells nuclei in CA1 and CA3 areas. Rats treated with Lithium-pilocarpine only revealed neuronal cell degeneration with neuroglial oedema and gliosis replacing ganglia cells. Co-administration of Lithium-pilocarpine and FP (50 – 200 mg/kg) showed protection and restoration of the CA1 and CA3 neural fibrillary processes and ganglia (Photomicrographs I – IV). A significant ($F_{4, 14}$ = 18.81, p = 0.0001; +++p < 0.001) reduction in hippocampal neurons was observed in CA1 of rats treated with Lithium-pilocarpine only, while concurrent treatments with FP and with Lithium-pilocarpine significantly ($F_{4, 14}$ = 18.81, p = 0.0001; *p < 0.05) increased the neuronal cells counts (Figure 5A). Similarly, Treatments with Lithium-pilocarpine only significantly [($F_{4, 14}$ = 41.49, p < 0.0001; +++p < 0.001) reduced the quantity of hippocampal neurons in the CA3, which were significantly [($F_{4, 14}$ = 41.49, p < 0.0001; **p < 0.01; ***p < 0.001) increased with simultaneous administration of FP and with Lithium-pilocarpine (Figure 5B)

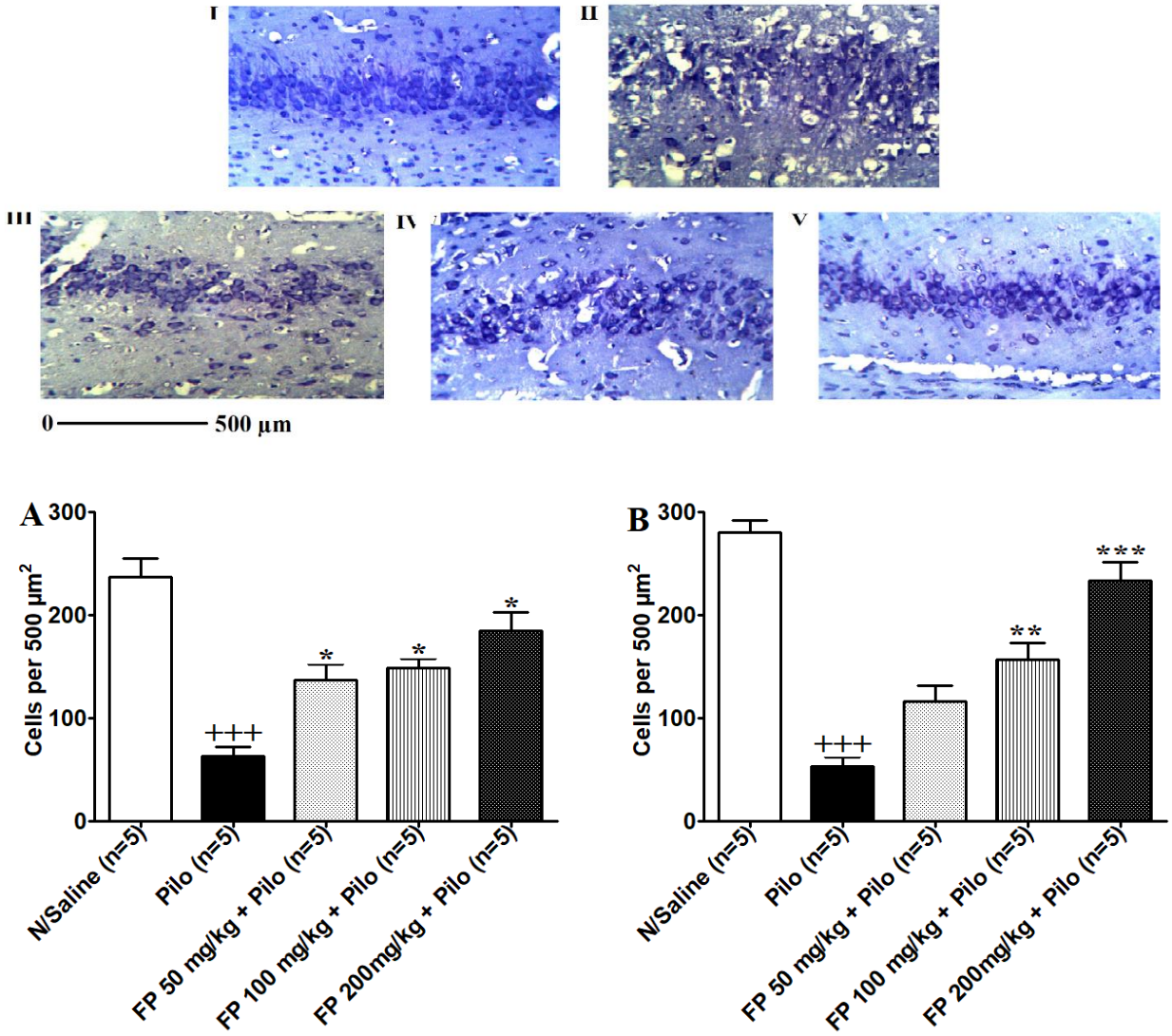

Figure 5: Effects of Ficus platyphylla (FP) on hippocampal neurons of rats treated with Lithium-pilocarpine. Photomicrographs of the dorsal hippocampus indicating, (I) Normal saline group showing normal neural processes and neuronal cells nuclei in CA1 and CA3 areas (Magnification × 400); (II) Rats treated with Lithium-pilocarpine only showing total replacement of the ganglia cells by neuroglial oedema and gliosis (Magnification × 400); (III) Rats treated with Lithium-pilocarpine and 50 mg/kg of FP showing fair preservation of the CA1 and CA3 neural fibrillary processes and ganglia (Magnification × 400); (IV) Rats treated with Lithium-pilocarpine and FP 100 mg/kg indicating preservation of the CA1 and CA3 neural fibrillary processes ganglia (Magnification × 400); (V) Rats treated with Lithium-pilocarpine and FP 200 mg/kg showing good preservation and restoration of the CA1 and CA3 neural fibrillary processes and ganglia. Effects of FP on the number of CA1 and CA3 neurons in the hippocampi of rats treated with Lithium-pilocarpine Histograms showing, (A) CA1 [($F_{4, 14}$ = 18.81, p = 0.0001; +++p < 0.001 (N/Saline vs Pilo), *p < 0.05 (Pilo vs FP 50 mg/kg + Pilo +; Pilo vs FP 100 mg/kg + Pilo +; Pilo vs FP 200 mg/kg + Pilo)]. (B) CA3 [($F_{4, 14}$ = 41.49, p < 0.0001; +++p < 0.001 (N/Saline vs Pilo), **p < 0.01 (Pilo vs FP 100 mg/kg + Pilo); ***p < 0.001 (Pilo vs FP 200 mg/kg + Pilo)]. Data expressed as Mean ± SE. n number of animals per group.

Molecular docking studies

Molecular docking techniques were employed to assess the interactions of 2, 3-dimethylphenylisothiocyanate, pentadecanoic acid and 11-octadecenoic acid with proteins to predict their binding manners to $GABA_{AT}$ and GAD active sites. The docking protocol was validated by re-docking the co-crystallized ligands (PLP in $GABA_{AT}$, PDB ID: 1OHV, and PLZ in GAD, PDB ID: 2OKJ). The re-docking reproduced the experimental binding orientations with strong binding affinities (PLP: –8.00 kcal/mol, Ki =

1.36 µM; PLZ: –8.97 kcal/mol, Ki = 264.97 nM; accompanied by hydrogen bonds), confirming the reliability of the docking parameters (Table 3 and Figure 6A). PLP interacts with eight (8) GABA protein residues in the active site: GLY 136, SER 137, SER 173, ASN 140, ASP 298, GLN 301, SER 325, and LYS 329 (Table 3 and Figure 7A). When benchmarked against these controls, the test ligands demonstrated lower binding energies and weaker inhibition constants. For example, 2,3-dimethylphenylisothiocyanate bound to $GABA_{AT}$ at –6.47 kcal/mol (Ki = 17.99 µM) and to GAD at –5.48 kcal/mol (Ki = 96.25 µM), indicating reduced affinity compared to the controls (Figure 6C). Similarly, Pentadecanoic acid and Octadecanoic acid showed binding energies between –5.25 and –5.86 kcal/mol (Figure 6B), with inhibition constants ranging from 50.65 to 141.27 µM across both proteins (Figure 6D and C). These compounds exhibited hydrogen bonding and a network of hydrophobic contacts. For instance, 2, 3-dimethylphenylisothiocyanate, H-bonds are formed between the ligand and GLN 301 and LYS 329 of the GABA active site (Figure 7B), which is comparable to the interaction site of the control dock. Furthermore, octadecanoic acid demonstrated only one H-bond contact at GLY 136 (Figures 6B and 7C), which was identical to the interaction of its control dock. Notably, pentadecanoic acid interacts with $GABA_{AT}$, with docking data indicating primarily hydrophobic interactions (Table 3 and Figure 6DG). GAD and PLZ crystal structures (2OKI) provided the best evidence as a control dock (Table 3) for identifying the involvement of ligands/tested molecules in GABA synthesis. The GAD-PLZ (receptor-ligand) complex is majorly held together by H-bond interactions with amino acid residues GLN 190, LEU 191, GLY 252, ALA 253, HIS 291, THR 348, ASP 373, and ASN 402 (Figure 7D), with a binding energy of -8.97 kcal/mol (Figure 6E). In contrast, the binding energy of 2, 3-dimethylphenylisothiocyanate was estimated to be -5.48 kcal/mol (Figure 6G), which was lower than the 2OKI control dock study but better than the variants of the molecules tested. However, the interacting molecule differs from the control dock, which creates an H-bond (Table 3). Pentadecanoic acids and octadecanoic acid, were found to have binding energies of about -5.31 and 5.25 kcal/mol, respectively (Figures 6F and 6H). These molecules exhibited identical H-bond interactions with GLN 190B and LEU 191B (Figure 7F) as pentadecanoic acids, which is analogous to the two-site interaction in the control dock. Furthermore, octadecanoic acid interacts with the GAD active site via GLY 252 and ASN 402 to create H-bonds (Figure 7E), which are also observed in the control dock. There are several hydrophobic interactions detected in the GC-MS compounds that were also observed in the control dock (Table 3). Apart from the H-bond and hydrophobic interactions observed in this study, salt bridges did occur in 1OHV and 2OKJ proteins (Table 3). Salt bridges are known to aid stabilizing enzyme-ligand complexes by acting as molecular clips that maintain the protein structures' shape together [53]. Here, a 1OHV study shows a phosphate-bridge formed between PLP with LYS 329 in the control dock. A different salt bridge carboxylate was observed in octadecanoic acid and pentadecanoic acid compounds formed between LYS 329 and ARG 192, respectively. Similar interaction on the benchmark 2OKJ, but with two salt bridges phosphate and carboxylate were formed between the compound PLZ and HIS 404 and ARG 567, respectively. However, only octadecanoic acid from the tested molecules formed a carboxylate salt bridge between the compound and HIS 404 (Table 3). Comparative interaction profiling revealed that the control ligands established several stable hydrogen bonds and hydrophobic interactions within the active sites. In contrast, the test compounds formed fewer hydrogen bonds and had less extensive hydrophobic interactions. PLP for instance, managed to create up to eight hydrogen bonds with residues like GLY136, SER137, and ASN140 in $GABA_{AT}$, while the test ligands formed one or two hydrogen bonds at longer distances. A similar pattern emerged with PLZ in GAD, which also formed eight hydrogen bonds along with multiple stabilizing hydrophobic contacts, whereas the test compounds showed fewer interactions. These findings highlight that the compounds studied do bind within the active sites with notably weaker affinity and interaction networks compared to the validated inhibitors.

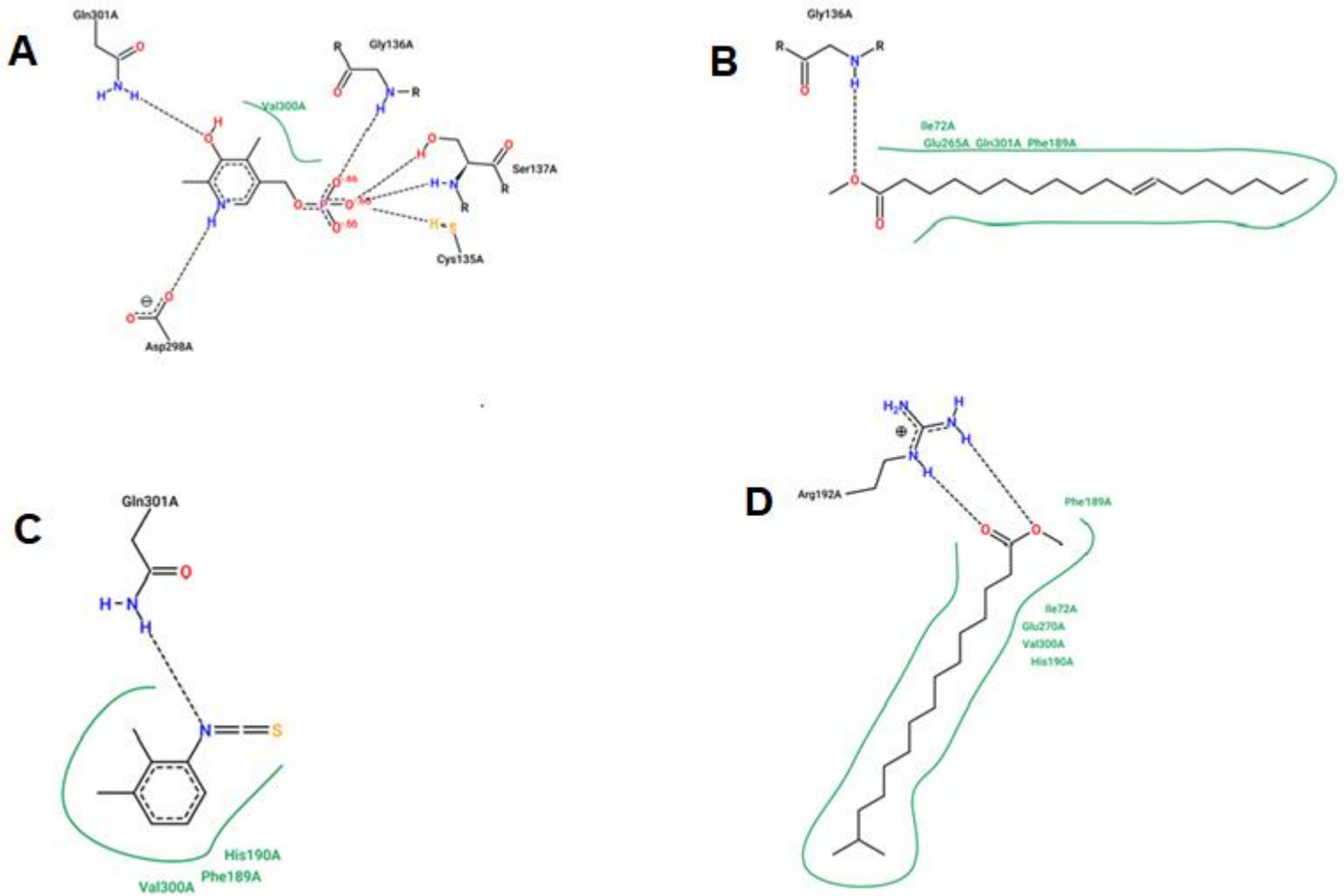
A
Gln301A
Gly136A
Val300A
Ser137A
Cys135A
Asp298A
B
Gly136A
Ile72A
Glu265A Gln301A Phe189A
C
Gln301A
His190A
Phe189A
Val300A
D
Arg192A
Phe189A
Ile72A
Glu270A
Val300A
His190A

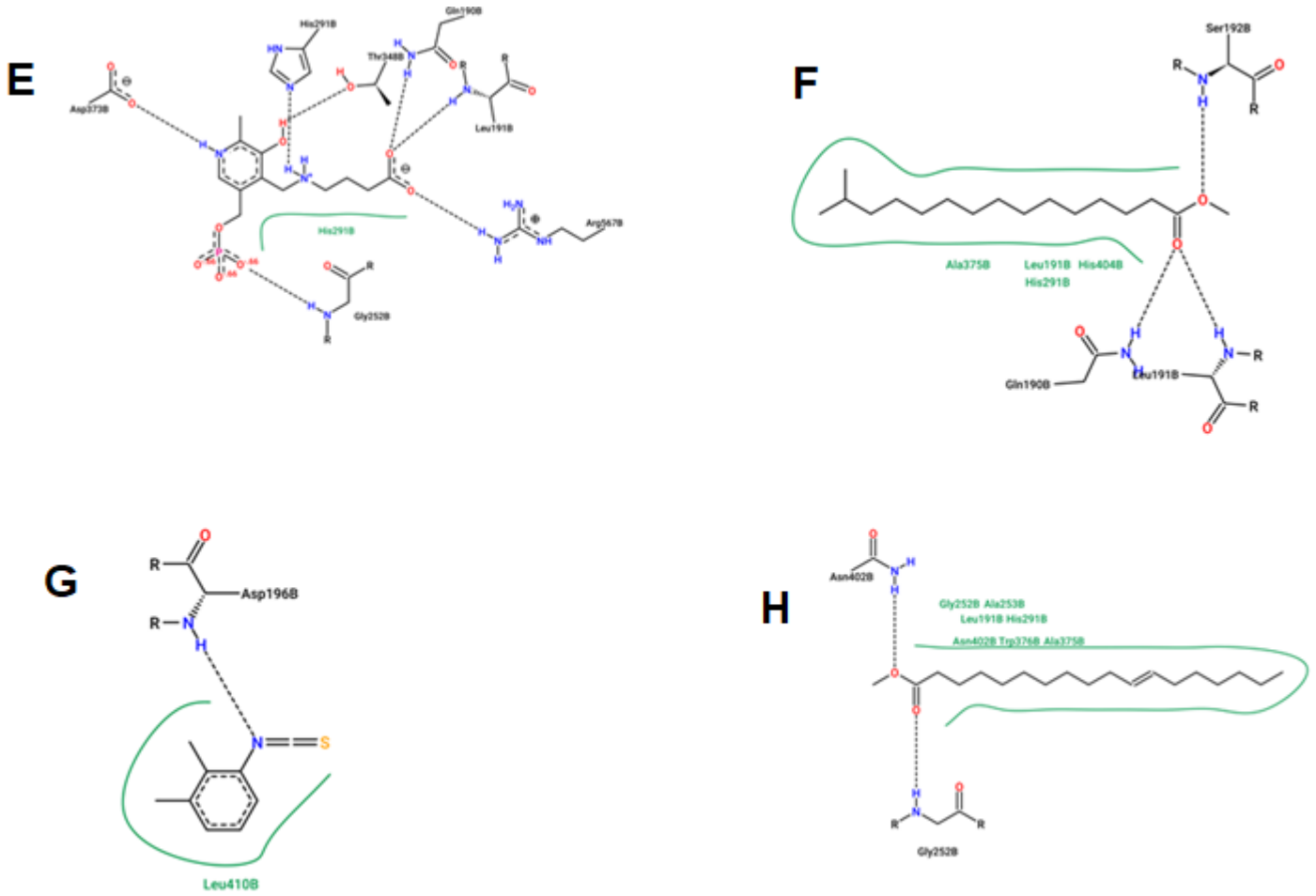

Figure 6: Figures (**A–D**) depict two-dimensional diagrams of complexes produced between $GABA_{AT}$ (1OHV) sites and the tested compounds, with hydrogen bonds in dotted lines and hydrophobic interaction areas in green. Binding sites found in the PLP control dock (**A**), as well as interactions of octadecanoic acid (**B**), 2, 3-dimethylphenylisothiocyanate (**C**), and pentadecanoic acids (**D**) with $GABA_{AT}$ protein. Figures (**E–H**) shows two-dimensional diagrams of complexes generated between GAD (2OKJ) sites and the tested compounds, illustrating hydrogen bonding in dotted lines and hydrophobic interaction areas in green colors. Binding sites found in the PLZ control dock (**E**), as well as interactions of pentadecanoic acids (F), 2, 3-dimethylphenylisothiocyanate (**G**), and octadecanoic acid (**H**) with GAD protein. All tested compounds demonstrated interactions with Gamma-aminobutyric acid aminotransferase ($GABA_{AT}$) and 2OKJ: Glutamic acid decarboxylase (GAD) (Table 3).

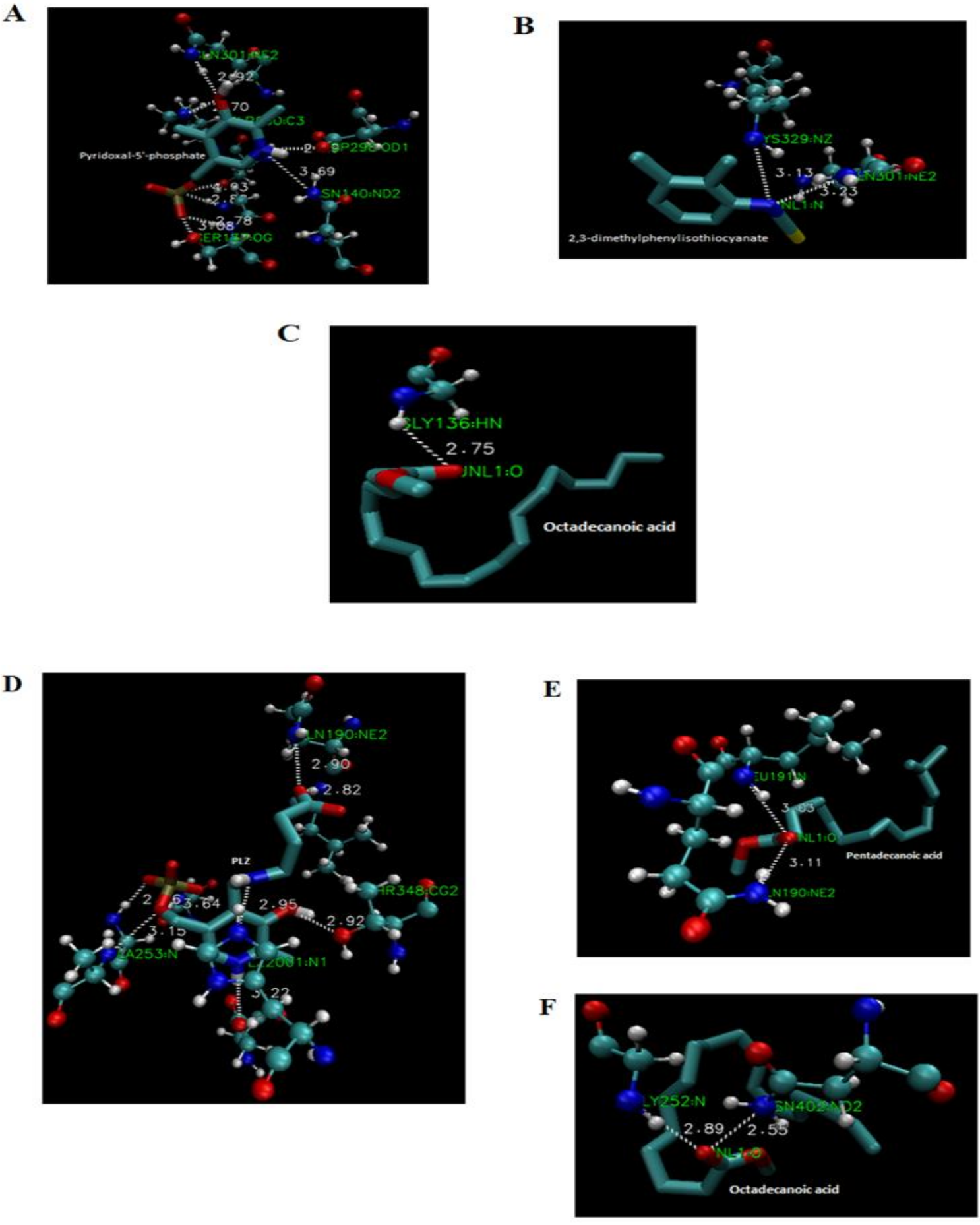
A
Pyridoxal-5'-phosphate
2.92
3.69
B
YS329:NZ
3.13
3.23
2,3-dimethylphenylisothiocyanate
C
LY136:HN
2.75
Octadecanoic acid
D
LN190:NE2
2.90
2.82
PLZ
2.95
2.92
3.15
E
3.03
3.11
Pentadecanoic acid
F
2.89
2.55
Octadecanoic acid

Figure 7: $GABA_{AT}$ (1OHV) docking with its crystal structure ligand and tested molecules. **(A)** Control dock showing hydrogen bond forming between PLZ and GLY136, SER137, SER173, ASN140, ASP298, GLN301, SER325, LYS329. (**B**) Hydrogen bond formation between 2, 3-dimethylphenylisothiocyanate, GLN301, and LYS329. (**C**) A hydrogen bond is formed between Octadecanoic acid and GLY136. GAD (2OKI) docking with its crystal structure ligand and tested molecules. (**D**) Control dock demonstrating the formation of hydrogen bonds between PLZ and GLN190, LEU191, GLY252, ALA253, HIS291, THR348, ASP373, and ASN402. (**E**) Hydrogen bond formation between pentadecanoic acids, GLN190, and LEU191. (**F**) Hydrogen bond formation between octadecanoic acid, GLY252, and ASN402.

Table 3: Molecular docking results for all small molecules benchmarking $GABA_{AT}$ and GAD.

Protein	Ligand/Small molecule	Binding Energy (Kcal/Mol)	Inhibition/Activation Constant (K_i)	Molecules involved in H-Bond interaction(s)	H-Bond length	Molecules involved in Hydrophobic interaction(s)	Salt Bridges
1OHV	PLP (control dock)	-8.00	1.36 µM	N@GLY136A-O1P@LIG N@SER137A-O2P@LIG OG@SER173A-O2P@LIG ND2@ASN140A-N1@LIG OD1@ASP298A-N1@LIG NE2@GLN301A-O3@LIG OG@SER325A-O1P@LIG NZ@LYS329A-O3@LIG	1.89 1.82 2.22 3.1 1.96 2.0 3.25 2.07	CE1@PHE189A-C4A@LIG CB@VAL300A-C2A@LIG CG1@VAL300A-C4@LIG CD@LYS329A-C4A@LIG	NZ@LYS329B-Phosphate@LIG
	2,3-dimethylphenylisothiocyanate	-6.47	17.99 µM	NE2@GLN301A - N@LIG NZ@LYS329A-N@LIG	3.23 3.13	CE1@PHE189A-C@LIG CB@VAL300A-C@LIG CG1@VAL300A-C@LIG	
	Octadecanoic acid	-5.86	50.65 µM	N@GLY136A-O@LIG	2.75	CG2@ILE72A-C@LIG CD1@PHE189A-C@LIG CZ@PHE189A-C@LIG CG@ARG192A-C@LIG CG@GLU265A-C@LIG CG@GLU270A-	NZ@LYS329B-Carboxylate@LIG

						C@LIG CB@VAL300A-C@LIG CG1@VAL300A-C@LIG CB@GLN301A-C@LIG CG2@THR302A-C@LIG	
	Pentadecanoic acids	-5.61	76.66 µM	-	-	CG2@ILE72A-C@LIG CE1@PHE189A-C@LIG CE1@PHE189A-C@LIG CG@GLU265A-C@LIG CG@GLU270A-C@LIG CB@VAL300A-C@LIG CG2@VAL300A-C@LIG CB@GLN301A-C@LIG CE@LYS329A-C@LIG	@ARG192A-Carboxylate@LIG
2OKJ	PLZ (Control dock)	-8.97	264.97 nM	NE2@GLN190B-O4@LIG N@LEU191B-O4@LIG N@GLY252B-O3P@LIG N@ALA253B-O4P@LIG NE2@HIS291B-N9@LIG	2.04 1.81 1.84 2.54 2.3 2.08 2.25 2.78	CG2@THR348B-C5@LIG CB@ALA375B-C2A@LIG	@HIS404B-Phosphate @ARG567B-Carboxylate@LIG

			OG1@THR348B-O3@LIG OD2@ASP373B-N1@LIG ND2@ASN402B-O4P@LIG			
2,3-dimethylphenylisothiocyanate	-5.48	96.25 µM	N@ASP196B-N@LIG	3.23	CD1@LEU195B-C@LIG CG@LEU410B-C@LIG CD1LEU411B-C@LIG	
Pentadecanoic acids	-5.31	128.84 µM	NE2@GLN190B-O@LIG N@LEU191B-O@LIG	3.11 3.03	CB@LEU191B-C@LIG CD2@LEU191B-C@LIG CB@HIS291B-C@LIG CG2@THR344B-C@LIG CB@ALA375B-C@LIG CB@TRP376B-C@LIG CB@ASN402B-C@LIG	
Octadecanoic acid	-5.25	141.27 µM	N@GLY252B-O@LIG ND2@ASN402B-O@LIG	2.89 2.55	CD2@LEU191B-C@LIG CB@HIS291B-C@LIG CG2@THR348B-C@LIG CB@ALA375B-C@LIG CB@ALA375B-C@LIG CB@TRP376B-	HIS404B-Carboxylate@LIG

		C@LIG CE3@TRP376B- C@LIG CB@ASN402B- C@LIG

Key: Protein crystal structures of – 1OHV: Gamma}-Aminobutyric Acid Aminotransferase ($GABA_{AT}$) and 2OKJ: Glutamic Acid Decarboxylase (GAD).

DISCUSSION

The present study revealed the ameliorative properties of *Ficus platyphylla's* (FP's) extract on lithium-pilocarpine-induced status epilepticus (SE) in rats. The extract *attenuated* lithium-pilocarpine-induced *oxidative stress,* seizure severity, and neuronal cell damage, and prolonged the latencies to seizures, and SE in non-protected rats. FP *increased the expression of genes encoding* glutathione-S-synthase (GSS), superoxide dismutase (SOD), catalase (CAT), and glutamic acid decarboxylase (GAD). Twenty biologically active secondary metabolites were detected in the methanol extract of FP by GC-MS analysis with the major constituents being 2, 3-dimethylphenylisothiocyanat (13.473%), pentadecanoic acid (13.1004%) and 11-Octadecenoic acid (14.3511%) given a total of 40.924% while the minor constituents constituted 59.08% These bioactive compounds play fundamental roles in excitatory amino acid receptor blockade, enhancement of cognitive functions, brain development and protection against oxidative damage, culminating in neuroprotective and anticonvulsant activities [2, 54, 55]. Molecular docking studies revealed interactions of these bioactive compounds with GAD and γ-aminobutyric acid aminotransferase ($GABA_{AT}$) active sites. In the present study, molecular docking was employed primarily to complement our biochemical, gene expression, and histological analyses. The docking results shed light on the interaction of the test compounds with the active sites of GAD and $GABA_{AT}$ through specific hydrogen bonds and hydrophobic contacts. Thus, predicting the ameliorative properties of FP on lithium-pilocarpine-induced status epilepticus. While additional mechanistic validation–like electrophysiological recordings, western blotting, or *in vivo* animal experiments–would certainly give more insights into the interactions, these were outside the scope of this study. Future research could build on these findings with such complementary experiments to offer a more in-depth mechanistic understanding.

The pilocarpine paradigm fulfills the criteria for an animal model of status epilepticus (SE). High-dose pilocarpine and Lithium-pilocarpine models produce indistinguishable behavioural, metabolic, neuropathological, and electrographic symptoms akin to human temporal lobe epilepsy [31, 56, 57]. Pilocarpine promotes uninterrupted excitatory and seizure activities, culminating in neuronal cell damage in the brain [58, 59]]. Lithium activates mononuclear cells and T-lymphocytes to potentiate the effects of pilocarpine, culminating in increased serum IL-1β levels, enhanced pilocarpine uptake, and altered blood-brain-barrier permeability [60]. Pre-treatment with LiCl increases acetylcholine release [61], with more acetylcholine crossing the synaptic cleft to the postsynaptic membrane where it activates M1 muscarinic receptors. The seizure initiation and propagation in pilocarpine-induced status epilepticus (SE) are intimately linked to increased *N*-methyl-D-aspartate (NMDA) and amino-3-hydroxy-5-methyl-4-isoxazolepropionic acid (AMPA) receptors, and decreased synaptic gamma-aminobutyric acid-$_A$ receptors ($GABA_ARs$) mediated neurotransmissions [31, 56, 57, 62]. Maladaptive synaptic trafficking mediated by $GABA_ARs$ and glutamate receptors contributes to pharmacoresistance to antiepileptic drugs and targeting these receptor complexes should ameliorate the pathophysiological consequences of refractory SE (RSE) [62].

In the present study, rats pretreated with Lithium chloride (LiCl) followed by pilocarpine injections demonstrated immobility, face clonus, head nodding, rearing and tumbling steadily progressing to generalized seizures, culminating in status epilepticus (SE). FP dose-dependently protected the rats from lithium-pilocarpine-induced status epilepticus (SE), significantly increased the Latency to status epilepticus in the non-protected rats, increased the Latency to seizures; and ameliorated seizure severity. The lithium–pilocarpine paradigm, which induces severe neuronal damage in the mesial structures, mossy fiber sprouting (MFS), hippocampal sclerosis, cell dispersion in the dentate gyrus (DG), and gliosis in the brain [7, 8], is a widely accepted model for acute SE and chronic TLE [63]. FP ameliorates Lithium-pilocarpine-induced SE by enhancement of synaptic gamma-aminobutyric acid-$_A$ receptors ($GABA_ARs$), and/or inhibition of amino-3-hydroxy-5-methyl-4-isoxazolepropionic acid (AMPA) and *N*-methyl-D-aspartate (NMDA) receptors mediated neurotransmissions or inhibition glutamate release [26, 62]. The bioactive compounds in FP demonstrated affinity for GABAergic and glutamatergic receptors, and a decrease in glutamate release in our previous binding studies [26].

Temporal lobe epilepsy (TLE) is associated with gliosis, mossy fiber sprouting, neuronal loss, expansion of the normally dense granule cell layer, or

atrophy predominantly in the dentate gyrus. CA1 and CA3 of the hippocampus [19]. The neuronal cell loss is typical of hippocampal sclerosis in TLE patients, and is believed to be the result of mitochondrial dysfunction, oxidative stress and overactivation of NMDARs culminating in excitotoxicity [64, 65, 66, 67], besides reduced glutamate uptake, enhanced glutamate release, calcium modulated NMDA currents, GABA receptor alterations, increase of cytokine expression, neuroplasticity modifications, and declined in glucose metabolism [2, 64, 68]. Histological evaluations showed alterations in neuronal cell densities in the CA1 and CA3 regions of rats injected with lithium-pilocarpine. Rats treated with Lithium-pilocarpine only revealed neuronal cell degeneration with mature adipocytes replacing ganglia cells, and fibrosclerosis observed in their brains. FP protected the hippocampal neuronal cell loss in lithium-pilocapine-induced SE rats by unknown and yet to be determined mechanism(s).

Neuroinflammation, oxidative stress and mitochondrial dysfunction are implicated in the pathogenesis of epilepsy. Oxidative stress ensuing from a disproportion between the production and elimination of reactive nitrogen species (RNS)/ reactive oxygen species (ROS) [69, 70, 71], accelerates neuronal damage, neuronal excitability and seizure onset by modulating Ca^{2+} homeostasis [72, 73]. Antioxidants protect cells from seizures' neurotoxic potentials [66, 74] and their combination with traditional AEDs or as monotherapy is becoming a major approach in the pharmacotherapy of epilepsy [75]. Antioxidants including N-acetylcysteine (NAC), polyphenols, lipoic acid, vitamin E, melatonin, and vitamin C effectively ameliorate oxidative-stress-associated neuronal damage and seizures in drug-resistant epilepsy [76, 77]. The present study evaluated the ameliorative properties of FP on biomarkers of oxidative stress as they modulate neuronal cell injury and seizure severity after lithium-pilocarpine-induced status epilepticus in rats. Seizures induce ROS/RNS generation, culminating in oxidative stress and cellular damage [78, 79]. The neuronal damage triggered by epileptic seizures is prevented by inhibition of ROS production [80, 81]. Reduced glutathione (GSH), catalase (CAT) and superoxide dismutase (SOD) are scavengers against oxidative stress, while malondialdehyde (MDA) produced by Lipid peroxidation connotes oxidative damage [82]. Rats injected with only lithium-pilocarpine in the present study revealed a significant increase in levels of MDA levels and a reduction in the GSH, CAT and SOD levels. Concurrent Pre-treatment with FP *increased the expression of genes encoding* glutathione-S-synthase (GSS), SOD, and CAT, decreased MDA levels and restored the antioxidant defense systems by increasing levels of GSH, SOD and CAT in the brains, thus demonstrating the benefits of FP in pharmacotherapy of epilepsy.

Modulation of γ-aminobutyric acid (GABA), synthesized from L-glutamate catalyzed by L-glutamic acid decarboxylase and degraded by the action of GABA aminotransferase (GABA-$_{AT}$), is pertinent in a plethora of neurological disorders [83]. A decrease in GABA levels, culminating in a down-regulation of inhibitory neurotransmission plays a pivotal role in the pathogenesis of epilepsy [83]. Inhibitors of GABA-$_{AT}$ are known to exhibit anticonvulsant property from a buildup of GABA concentration [84, 85]. Reduction in GAD activity is linked to several forms of treatment resistant epilepsy [86]. In this study, FP *increased the expression of genes encoding* glutamic acid decarboxylase (GAD), and molecular docking studies revealed interactions of the major bioactive compounds detected in the extract with GAD and γ-aminobutyric acid aminotransferase ($GABA_{AT}$) active sites.

Failure to isolate bioactive compounds of FP, the absence of other models of temporal lobe epilepsy and lack of simultaneously electroencephalogram (EEG) recordings from the hippocampus for validation as well as inability to select more representative brain regions associated with epileptic foci, rather than using whole brain tissue for biochemical experiments. Furthermore, paucity of additional evidence including Western blotting, electrophysiological data or animal experiments beyond seizure severity to better elucidate mechanism(s) of action of bioactive compounds in the extract, all constitute the limitations of your study.

CONCLUSION

The study validated the ameliorative potentials of FP on lithium-pilocarpine-induced status epilepticus (SE). The extract alleviated lithium–pilocarpine-induced neuronal cell damage, seizure severity, and alterations of *oxidative stress biomarkers.* FP prolonged the latencies to seizures and SE in non-protected rats, and increased *the expression of genes encoding* glutathione-S-synthase (GSS), superoxide dismutase (SOD), catalase (CAT), and glutamic acid

decarboxylase (GAD). Furthermore, the major bioactive compounds in the extract showed interactions with GAD and γ-aminobutyric acid aminotransferase ($GABA_{AT}$) active sites. These results are preliminary findings and additional studies are required to unravel the potential values of FP for the management of temporal lobe epilepsy.

Abbreviations

AEDs, Anti-epileptic Drugs; AMPARs, Amino-3-hydroxy-5-methyl-4-isoxazolepropionic acid receptors; ATPase, Adenosine triphosphatase; CAT, Catalase; CNS, Central nervous system; DG, Dentate gyrus; DTNB, 5, 5–dithiobis-(2-nitrobenzoic acid); FP, *Ficus platyphylla;* FT-IR, Fourier-transform infrared spectroscopy; GABA, γ–aminobutyric acid; $GABA_ARs$, γ–aminobutyric acid-$_A$ receptors; $GABA_{AT}$, γ-aminobutyric acid aminotransferase; GAD; Glutamic acid decarboxylase; GC-MS; Gas Chromatography-Mass Spectrometry; GSH, Glutathione; GSS, Glutathione-S-synthase; HPLC, High Performance Liquid Chromatography; LiCl, Lithium chloride; MDA, Malondialdehyde; MFS, mossy fiber sprouting; NAC, N-acetyl cysteine; NMDARs, *N*-methyl-D-aspartate receptors; qRT-PCR, Quantitative real-time PCR; RNS, Reactive nitrogen species; ROS, Reactive oxygen species; SE, Status epilepticus; SOD, Superoxide dismutase; SRSs, Spontaneous recurrent seizures; TIC, Total ion count; TLE, Temporal lobe epilepsy;

ACKNOWLEDGMENT

The technical assistance offered by personnel of the Department of Pharmacology and Toxicology, KASU, Kaduna, Nigeria, are hereby acknowledged.

AUTHORS' CONTRIBUTION

BAC: *conceived and designed experiments, conducted experiments, analyzed experimental data, drafted the manuscript.* MIY: *conducted experiments, reviewed and revised the Manuscript.* AAJ: *conducted experiments, reviewed and revised, the Manuscript.* NSS: *conducted experiments,* IA: *conducted experiments and analyzed experimental data,* PMW: *conducted experiments and analyzed experimental data,* SAJ: *conducted experiments and analyzed experimental data.* GIA: *conducted experiments, analyzed experimental data.* ZL: *conducted experiments and analyzed experimental data. SA*: supervised and *analyzed experimental data, reviewed and revised the Manuscript.*

CONFLICT OF INTEREST

The research was conducted without any potential conflicts of interest.

FUNDING

The Kaduna State University (KASU), Kaduna, Nigeria, and the Tertiary Education Trust Fund (TETFund) Nigeria (TETF/DR&D/UNI/KADUNA/IBR/2022; Batch 4) jointly funded this study.

REFERENCES

1. Fisher RS, van Em de Boas W, Blume W, Elger C, Genton P, Lee P, Engel J. "Epileptic seizures and epilepsy: definitions proposed by the International League against Epilepsy (ILAE) and the International Bureau for Epilepsy (IBE)". Epilepsia, 46, 2005:470–472. doi.org/10.1111/j.0013-9580.2005.66104.x
2. Chindo BA, Yakubu MI, Jimoh AA, Waziri PM, Abdullahi I, Ayuba GI, Becker A. *Ficus platyphylla* alleviates seizure severity and neurobehavioral comorbidities in pentylenetetrazole–kindled rats via modulation of oxidative stress. Brain Research, 1838, 2024: 148994. doi: 10.1016/j.brainres.2024.148994.
3. Scott RC, Surtees RAH, Neville BGR. Status epilepticus: pathophysiology, epidemiology, and outcomes. Archives of Disease Childhood, 79, 1998: 73–77. doi: 10.1136/adc.79.1.73.
4. Brown JK, Hussain IA. Status epilepticus. I: Pathogenesis. Developmental Medicine & Child Neurology, 33, 1991: 3–17. doi: 10.1111/j.1469-8749.1991.tb14780.x.
5. Haglid KG, Wang S, Qiner Y, Hamberger A. Excitotoxicity. Experimental correlates to human epilepsy. Molecular Neurobiology, 9, 1994: 259–263. doi: 10.1007/BF02816125.
6. Fountain NB, Lothman EW. Pathophysiology of status epilepticus. Journal of Clinical Neurophysiology, 12, 1995: 326–342. PMID: 7560021
7. Curia G, Longo D, Biagini G, Jones R, Avolia M. The pilocarpine model of temporal lobe epilepsy. Journal of Neuroscience Methods, 172, 2008: 143–157. doi: 10.1016/j.jneumeth.2008.04.019

8. Kandratavicius L, Balista PA, Lopes-Aguiar C, Ruggiero RN, Umeoka EH, Garcia-Cairasco N, *et al*., Animal models of epilepsy: use and limitations. Neuropsychiatric Disease and Treatment, 10, 2014: 1693–1705. doi: 10.2147/NDT.S50371.
9. Ji D, Mylvaganam S, Ravi Chander P, Tarnopolsky M, Murphy K, Carlen P. Mitochondria and oxidative stress in epilepsy: advances in antioxidant therapy. Frontiers in Pharmacology, 15, 2025: 1505867. doi.org/10.3389/fphar.2024.1505867
10. Lopriore P, Gomes F, Montano V, Siciliano G, Mancuso M. Mitochondrial epilepsy, a challenge for neurologists. International Journal of Molecular Sciences, 23, 2022: 13216. doi: 10.3390/ijms232113216.
11. Kapron B, Czarnomysy R, Wysokinski M, Andrys R, Musilek K, Angeli A, Supuran CT, Plech T. 1,2,4-Triazole-based anticonvulsant agents with additional ROS scavenging activity are effective in a model of pharmacoresistant epilepsy. Journal of Enzyme Inhibition and Medicinal Chemistry, 35, 2020: 993–1002. doi.org/10.1080/14756366.2020.1748026
12. Parsons ALM, Bucknor EMV, Castroflorio E, Soares TR, Oliver PL, Rial D. The interconnected mechanisms of oxidative stress and neuroinflammation in epilepsy. Antioxidants, 11, 2022: 157. doi: 10.3390/antiox11010157.
13. Juan CA, Pérez De La Lastra JM, Plou FJ, Pérez-Lebeña E. The chemistry of reactive oxygen species (ROS) revisited: outlining their role in biological macromolecules (DNA, lipids and proteins) and induced pathologies. International Journal of Molecular Sciences, 22, 2021: 4642. doi:10.3390/ijms22094642
14. Kowalczyk P, Sulejczak D, Kleczkowska P, Bukowska-Ośko I, Kucia M, Popiel M, et al., Mitochondrial oxidative stress-A causative factor and therapeutic target in many diseases. International Journal of Molecular Sciences, 22, 2021: 13384. doi: 10.3390/ijms222413384.
15. Pizzino G, Irrera N, Cucinotta M, Pallio G, Mannino F, Arcoraci V, et al., Oxidative stress: harms and benefits for human health. Oxidative Medicine and Cellular Longevity, 2017: 8416763. doi: 10.1155/2017/8416763.
16. Yilgor A, Demir C. Determination of oxidative stress level and some antioxidant activities in refractory epilepsy patients. Science Reports, 14, 2024: 6688. doi.org/10.1038/s41598-024-57224-6
17. Cardenas-Rodriguez N, Huerta-Gertrudis B, Rivera-Espinosa L, MontesinosCorrea H, Bandala C, Carmona-Aparicio L, et al., Role of oxidative stress in refractory epilepsy: evidence in patients and experimental models. International Journal of Molecular Sciences, 14, 2013: 1455–1476. doi: 10.3390/ijms14011455.
18. Kurita T, Sakurai K, Takeda Y, Horinouchi T, Kusumi I. Very long-term outcome of non-surgically treated patients with temporal lobe epilepsy with hippocampal sclerosis: A Retrospective study. PLoS One, 11, 2016: e0159464. doi: 10.1371/journal.pone.0159464.
19. McIntosh WC, Joe MD. Temporal seizures; National library of medicine. Start Pearls Publishing LLC. PMID: 31751042. (2023).
20. Bum EN, Schmutz M, Meyer C, Rakotonirina A, Bopelet M, Portet C, Jeker A, Rakonirina SV, Olpe HR, Herrling P. Anticonvulsant properties of the methanolic extracts of *Cypeus articulatus* (Cyperaceae), Journal of Ethnopharmacology, 76, 2001: 145–150. doi: 10.1016/s0378-8741(01)00192-1.
21. Bienvenu E, Amabeoku GJ, Eagles PK, Scott G, Springfield EP. Anticonvulsant activity of aqueous extract of *Leonotis leonurus*. Phytomedicine, 9, 2002: 217–223. doi: 10.1078/0944-7113-00103.
22. Adeyemi OO, Yemitan OK, Adebiyi OO. Sedative and anticonvulsant activities of the aqueous root extract of *Sanseviera liberica* Gerome & Labroy (Agavaceae). Journal of Ethnopharmacology, 113, 2007: 111–114. doi: 10.1016/j.jep.2007.05.007.
23. Ojewole JA. Anticonvulsant activity of *Hypoxis hemerocallidea* Fisch. & C. A. Mey. (Hypoxidaceae) corm ('African potato') aqueous extract in mice. Phytotherapy Research, 22, 2008: 91–96. doi: 10.1002/ptr.2272.
24. Chindo BA, Anuka JA, McNeil L, Yaro AH, Adamu SS, Amos S, Connelly WK, Lees G, Gamaniel KS. Anticonvulsant properties of

saponins from *Ficus platyphylla* stem bark. Brain Research Bulletin, 78, 2009: 276–282. doi: 10.1016/j.brainresbull.2008.12.005.

25. Chindo BA, Ya'U J, Danjuma NM, Okhale SE, Gamaniel KS, Becker A. Behavioral and anticonvulsant effects of the standardized extract of *Ficus platyphylla* stem bark. Journal of Ethnopharmacology, 154, 2014: 351–360. doi: 10.1016/j.jep.2014.03.061.
26. Chindo BA, Schroder H, Becker A. Methanol extract of *Ficus platyphylla* ameliorates seizure Severity, cognitive deficit and neuronal cell loss in pentylenetetrazole kindled mice. Phytomedicine, 22, 2015: 86–93. DOI: 10.1016/j.phymed.2014.10.005
27. Chindo BA, Anuka JA, Gamaniel KS. Toxicity screenings of *Ficus platyphylla* stem bark in rats. Pharmacologia, 3, 2012: 499 – 505. doi=pharmacologia.2012.499.505
28. Beschi DA, Appavoo MR, Irene Wilsy JI. GC-MS analysis, collected from Kavalkinaru area, Tirunelveli District, Tamil Nadu, India. European Journal of Molecular & Clinical Medicine, 8, 2021: 4287–4292.
29. Ahmad M. Protective effects of curcumin against lithium–pilocarpine induced status epilepticus, cognitive dysfunction and oxidative stress in young rats. Saudi Journal of Biological Sciences, 20, 2013: 155–162. doi: 10.1016/j.sjbs.2013.01.002.
30. Fan J, Shan W, Yang H, Zhu F, Liu X, Wang Q. Neural activities in multiple rat brain regions in lithium-pilocarpine-induced status epilepticus model. Frontier in Molecular Neuroscience, 12, 2020: 323. doi.org/10.3389/fnmol.2019.00323
31. Clifford DB, Olney JW, Maniotis A, Collins RC, Zorumski CF. The functional anatomy and pathology of lithium-pilocarpine and high-dose pilocarpine seizures. Neuroscience, 23, 1987: 953–968. doi: 10.1016/0306-4522(87)90171-0.
32. Vezzani A. Pilocarpine-induced seizures revisited: what does the model mimic? Epilepsy Currents, 9, 2009: 146–148. doi: 10.1111/j.1535-7511.2009.01323.x
33. Persinger MA, Bureau YRJ, Kostakos M, Peredery O, Falter H. Behaviors of rats with insidious multifocal brain damage induced by seizures following single peripheral injections of lithium and pilocarpine. Physiology and Behavior, 53, 1993: 849–856. doi: 10.1016/0031-9384(93)90261-d.
34. Imran I, Hillert MH, Klein J. Early metabolic responses to lithium/pilocarpine-induced status epilepticus in rat brain. Journal of Neurochemistry, 135, 2015: 1007–1018. doi: 10.1111/jnc.13360.
35. Modebadze T, Morgan NH, Pérès IA, Hadid RD, Amada N, Hill C, Williams C, Stanford IM, Morris CM, Jones RS, Whalley BJ, Woodhall GL. A low mortality, high morbidity reduced intensity status epilepticus (RISE) model of epilepsy and epileptogenesis in the rat. PloS One, 11, 2016: e0147265. doi: 10.1371/journal.pone.0147265.
36. Kow RI, Kelly Alipi KJ, Naydenov V, Le JH, Stella N, Neil M, Nathanson NM. Modulation of pilocarpine-induced seizures by cannabinoid receptor 1. PLoS One, 9, 2014: e95922. doi: 10.1371/journal.pone.0095922.
37. Moron MS, Depierre JW, Mannervik B. Levels of glutathione, glutathione reductase and glutathione S-transferase activities in rat lung and liver. Biochim Biophys Acta, 582, 1979: 67–78. doi: 10.1016/0304-4165(79)90289-7.
38. Ohkawa H, Ohishi N, Yagi K. Assay for lipid peroxides in animal tissues by thiobarbituric acid reaction. Analytical Biochemistry, 95, 1979: 351–358. doi: 10.1016/0003-2697(79)90738-3.
39. Misra HP, Fridovich I. The role of superoxide anion in the anti-oxidation of epinephrine and simple assay for superoxide dismutase. Journal of Biological Chemistry, 247, 1972: 3170–3175. doi.org/10.1016/S0021-9258(19)45228-9.
40. Goth LA. Simple method for determination of serum catalase activity and revision of reference range. Clinica Chimica Acta, 196, 1991: 143–151. doi: 10.1016/0009-8981(91)90067-m.
41. Livak KJ, Schmittgen TD. Analysis of relative gene expression data using real-time quantitative PCR and the 2(-Delta Delta C(T)) method. Methods, 25, 2001: 402–408. doi: 10.1006/meth.2001.1262.
42. Rao, X. Huang, Z. Zhou, X.X. Lin, An improvement of the 2ˆ(–delta delta CT) method for quantitative real-time polymerase chain reaction data analysis. Biostatistics,

Bioinformatics and Biomathematics, 3, 2013: 71–85. PMCID: PMC4280562

43. Waziri P, Auta R, Imam MU, Chindo BA, Ladan Z, Mohammed Z, Wayah S, Mohammed J, Tahir MI, Ahmad AE, Alhassan Y, Tyoapine D, Agbaji AS. *In vivo* anti-hepatocellular carcinoma effects of the chloroform root extract of *Clausena excavata Burm*. Journal Evidence-Based Integrative Medicine, 29, 2024: 1–8. doi: 10.1177/2515690X241251558.
44. James SA, Yam WK. 'Sub-structure-based screening and molecular docking studies of potential enteroviruses inhibitors. Computational Biology and Chemistry, 92, 2021: 107499. doi: 10.1016/j.compbiolchem.2021.107499.
45. Meng XY, Zhang HX, Mezei M, Cui M. Molecular docking: a powerful approach for structure-based drug discovery. Current Computer-aided Drug Design, 7, 2011: 146–157. doi: 10.2174/157340911795677602
46. Kim S, Chen J, Cheng T, Gindulyte A, He J, He S, Li Q, Shoemaker BA, Thiessen PA, Yu B, Zaslavsky L, Zhang J, Bolton EE. PubChem 2025 update. Nucleic Acids Research, 53(D1), 2025: D1516 – D1525. doi.org/10.1093/nar/gkae1059
47. O'Boyle NM, M. Banck M, C.A. James CA, C. Morley C, T. Vandermeersch T, G.R. Hutchison GR. Open Babel: An open chemical toolbox. Journal of Cheminformatics, 3(1), 2011: 33. doi: 10.1186/1758-2946-3-33.
48. Morris GM et al., 'AutoDock4 and AutoDockTools4: Automated docking with selective receptor flexibility', Journal of Computational Chemistry, 30, 2009: 2785–2791. doi.org/10.1002/jcc.21256
49. Salentin S et al., PLIP: fully automated protein–ligand interaction profiler. Nucleic Acids Research, 43(W1), 2015: W443–W447. doi: 10.1093/nar/gkv315.
50. Schöning-Stierand K, Diedrich K, Ehrt C, Flachsenberg F, Graef J, Sieg J, Penner P, Poppinga M, Ungethüm A, Rarey M. ProteinsPlus: a comprehensive collection of web-based molecular modeling tools. Nucleic Acids Research, 50(W1), 2022: W611–W615. doi: 10.1093/nar/gkac305.
51. Stierand K, Rarey M. From modeling to medicinal chemistry: automatic generation of two-dimensional complex diagrams. ChemMedChem, 2, 2007: 853–860. doi: 10.1002/cmdc.200700010.
52. Stierand K, Rarey M. Drawing the PDB: Protein−ligand complexes in two dimensions. ACS Medicinal Chemistry Letters, 1, 2010: 540–545. doi.org/10.1021/ml100164p
53. Spassov DS, Atanasova M, Doytchinova L. A role of salt bridges in mediating drug potency: A lesson from the N-myristoyltransferase inhibitors. Frontiers in Molecular Biosciences, 9, 2023: 1066029. doi.org/10.3389/fmolb.2022.1066029.
54. Wang Z, Li G, Tang W, Yin M. Neuroprotective effects of stearic acid against toxicity of oxygen/glucose deprivation or glutamate on rat cortical or hippocampal slices. Acta Pharmacologica Sinica, 27, 2006: 145–150. DOI:10.1111/j.1745-7254.2006.00259.x
55. Hussain G, Schmitt F, Loeffler J-P, Gonzalez de Aguilar J-L. Fatting the brain: a brief of recent research. Front. Cell. Neurosci, 7, 2013: 144. DOI: 10.3389/fncel.2013.00144
56. Juvale IIA, Has ATC. The evolution of the pilocarpine animal model of status epilepticus. Heliyon 6, 2020: e04557. doi: 10.1016/j.heliyon.2020.e04557.
57. Müller CJ, Bankstahl M, Groticke I, L € oscher W. Pilocarpine vs. lithium–pilocarpine for induction of status epilepticus in mice: development of spontaneous seizures, behavioral alterations and neuronal damage. European Journal of Pharmacology, 619, 2009: 15–24. doi: 10.1016/j.ejphar.2009.07.020.
58. Bymaster F, Carter P, Yamada M, Gomeza J, Wess J, Hamilton S, Nathanson N, McKinzie D, Felder C. Role of specific muscarinic receptor subtypes in cholinergic parasympathomimetic responses, in vivo phosphoinositide hydrolysis, and pilocarpine-induced seizure activity. European Journal of Neuroscience, 17, 2003: 1403–1410. doi: 10.1046/j.1460-9568.2003.02588.x.
59. Lee M, Choi B, Suh S. Unexpected effects of acetylcholine precursors on pilocarpine seizure-induced neuronal death. Current Neuropharmacology, 16, 2018: 51–58. doi: 10.2174/1570159X15666170518150053.

60. Marchi N, Fan Q, Ghosh C, Fazio V, Bertolini F, Betto G, Batra A, Carlton E, Najm I, Granata T, Janigro D. Antagonism of peripheral inflammation reduces the severity of status epilepticus. Neurobiol Dis, 33, 2009: 171–181. DOI: 10.1016/j.nbd.2008.10.002
61. Hillert M, Imran I, Zimmermann M, Lau H, Weinfurter S, Klein J. Dynamics of hippocampal acetylcholine release during lithium-pilocarpine-induced status epilepticus in rats. Journal of Neurochemistry, 131, 2014: 42–52. doi: 10.1111/jnc.12787.
62. Lumley L, Niquet J, Marrero-Rosado B, Schultz M, Franco Rossetti F, deA. Furtado M, Wasterlain C. Treatment of acetylcholinesterase inhibitor-induced seizures with polytherapy targeting GABA and glutamate receptors. Neuropharmacology, 185, 2021: 108444. doi: 10.1016/j.neuropharm.2020.108444.
63. Lévesque M, Avoli M, Bernard C. Animal models of temporal lobe epilepsy following systemic chemoconvulsant administration. Journal of Neuroscience Methods, 260, 2016: 45–52. doi: 10.1016/j.jneumeth.2015.03.009.
64. Chen SD, Chang AY, Chuang YC. The potential role of mitochondrial dysfunction in seizure-associated cell death in the hippocampus and epileptogenesis. Journal of Bioenergetics and Biomembranes, 42, 2010: 461–465. doi: 10.1007/s10863-010-9321-8.
65. Puttachary S, Sharma S, Stark S, Thippeswamy T. Seizure-induced oxidative stress in temporal lobe epilepsy. BioMed Research International, 2015: 745613. doi: 10.1155/2015/745613.
66. Lin TK, Chen SD, Lin KJ, Chuang YC. Seizure-induced oxidative stress in Status epilepticus: is antioxidant beneficial? Antioxidants, 9, 2020: 1029. doi: 10.3390/antiox9111029
67. Carreño-González AJ, Liberato JL, Celani MVS, et al., Neuroprotective effects of chlorogenic acid against oxidative stress in rats subjected to lithium-pilocarpine-induced status epilepticus. Naunyn-Schmiedeberg's Arch Pharmacol (2024). doi: 10.1007/s00210-024-03080-0.
68. Chindo BA, Howes M–JR, S. Abuhamdah S, Yakubu MI, Ayuba GI, Battison A, Chazot PL. New insights into the anticonvulsant effects of essential oil from *Melissa officinalis* L. (lemon balm). Frontiers in Pharmacology, 12, 2021: 760674, 1–19. doi.org/10.3389/fphar.2021.760674.
69. Li S, Luo Z, Lu B, Xia S, Li C, Guan X, Zhang J, Huang K, Xian F. Protective effects of lycopene on kainic acid-induced seizures. *Epilepsy Research, 15, 2019:* 1–6. doi: 10.1016/j.eplepsyres.2019.01.010.
70. Jaiswal G, Kumar P. Neuroprotective role of apocynin against pentylenetetrazole kindling epilepsy and associated comorbidities in mice by suppression of ROS/RNS. *Behavioural Brain Research, 419,* **2022***:* 113699. doi: 10.1016/j.bbr.2021.113699.
71. Madireddy S, Madireddy S. Therapeutic interventions to mitigate mitochondrial dysfunction and oxidative stress-induced damage in patients with bipolar disorder. *International Journal of Molecular Sciences, 23, 2023:* 1844. doi: 10.3390/ijms23031844.
72. Yuen AW, Keezer MR, Sander JW. Epilepsy is a neurological and a systemic disorder. *Epilepsy and Behaviour, 78, 2018:* 57–61. doi: 10.1016/j.yebeh.2017.10.010.
73. Tashakori-Miyanroudi M, Ramazi S, Hashemi P, Nazari-Serenjeh M, Baluchnejadmojarad T, Roghani M. Acetyl-L–Carnitine exerts neuroprotective and anticonvulsant effect in kainate murine model of temporal lobe epilepsy. *Journal of Molecular Neuroscience, 72, 2022:* 1224–1233. doi: 10.1007/s12031-022-01999-8.
74. Liu YF, Gao F, Li XW, Jia RH, Meng XD, Zhao R, Jing YY, Wang Y, Jiang W. The anticonvulsant and neuroprotective effects of baicalin on pilocarpine-induced epileptic model in rats. Neurochemical Research, 37, 2012: 1670–1680. doi: 10.1007/s11064-012-0771-8.
75. Rizwana N, Agarwal V, Nune M. Antioxidant for neurological diseases and neurotrauma and bioengineering approaches. Antioxidants, 11, 2021: 72. doi.org/10.3390/antiox11010072
76. Sudha K, Rao AV, Rao A. Oxidative stress and antioxidants in epilepsy. *Clinica Chimica Acta, 303, 2001:* 19–24. doi: 10.1016/s0009-8981(00)00337-5.

77. Brookes PS, Yoon Y, Robotham JL, Anders MW, Sheu SS. Calcium, ATP, and ROS: A mitochondrial love-hate triangle. American Journal of Physiology-Cell Physiology*, 287, 2004:* C817–C833. doi: 10.1152/ajpcell.00139.2004.
78. Pisochi AM, Pop A. The role of antioxidants in the chemistry of oxidative stress: A review. European Journal of Medicinal Chemistry, *97, 2015:* 55–74. doi.org/10.1016/j.ejmech.2015.04.040
79. da Fonsêca DV, da Silva Maia Bezerra Filho C, Lima TC, de Almeida RN, de Sousa DP. Anticonvulsant Essential Oils and Their Relationship with Oxidative Stress in Epilepsy. *Biomolecules, 9,* 2019*:* 835. doi: 10.3390/biom9120835
80. Williams S, Hamil N, Abramov AY, Walker MC, Kovac S. Status epilepticus results in persistent overproduction of reactive oxygen species: Inhibition of which is neuroprotective. *Neuroscience 303, 2015:* 160–165. doi: 10.1016/j.neuroscience.2015.07.005.
81. Sandouka S, Shekh-Ahmad T. Induction of the Nrf2 pathway by sulforaphane is neuroprotective in a rat temporal lobe epilepsy model. *Antioxidants, 10,* 2021*:* 1702. doi: 10.3390/antiox10111702.
82. Singh N, Vijayanti S, Saha L, et al., Neuroprotective effect of Nrf2 activator dimethyl fumarate, on the hippocampal neurons in chemical kindling model in rat. Epilepsy Research, 143, 2018: 98–104. doi: 10.1016/j.eplepsyres.2018.02.011.
83, Park J-Y, Lee Y, Lee HJ, Kwon Y-S, Chun W. *In silico* screening of GABA aminotransferase inhibitors from the constituents of *Valeriana officinalis* by molecular docking and molecular dynamics simulation study. Journal of Molecular Modeling, 26, 2020: 228. doi: 10.1007/s00894-020-04495-1.
84. Nanavati SM, Silverman RB. Design of potential anticonvulsant agents: mechanistic classification of GABA aminotransferase inactivators. Journal of Medicinal Chemistry, 32, 1989:2413–2421. doi: 10.1021/jm00131a001.
85. Silverman RB. Mechanism-based enzyme in activators. Methods in Enzymology, 249, 1995: 240–283. doi: 10.1016/0076-6879(95)49038-8.
86. Zhang Y, Vanmeert M, Siekierska A, Ny1 A, John J, Callewaert G, Lescrinier E, Dehaen W, de Witte PAM, Kaminski RM. Inhibition of glutamate decarboxylase (GAD) by ethyl ketopentenoate (EKP) induces treatment-resistant epileptic seizures in Zebra fish. Scientific Reports, 7, (2017: 7195. doi: 10.1038/s41598-017-06294-w.